

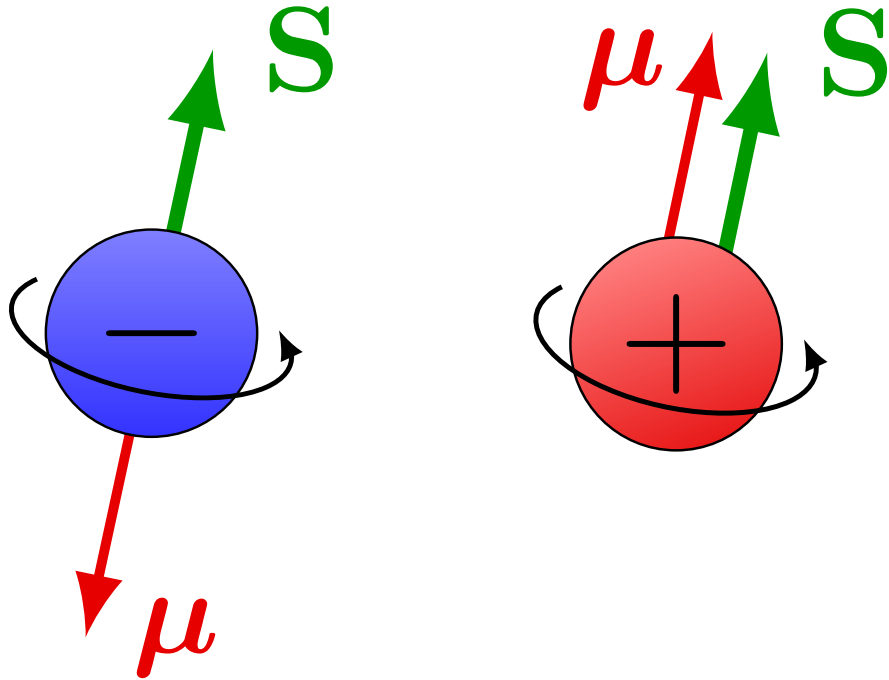
**First observation of  $\gamma\gamma \rightarrow \tau\tau$  in pp collisions**

**Constraints on  $\tau$  electromagnetic moments**

Cécile Caillol, CERN

LPCC seminar, March the 12<sup>th</sup> 2024

# Lepton magnetic moment



$$\mu = g \frac{e}{2m} \mathbf{S}$$

- Spin and magnetic moment of lepton related via gyromagnetic factor  $g$
- Dirac equation predicts  $g = 2$

# Lepton anomalous magnetic moment

- In QED, quantum effects modify the value of  $g$ , giving rise to an anomalous magnetic moment:

$$a_\ell = (g - 2) / 2$$

- NLO prediction (Schwinger, 1948):

$$a_\ell = \alpha / 2\pi \cong 0.00116$$

- Further corrections calculated



# $a_\ell$ measurements

## Electron

- One of the most precisely measured quantities in physics
- Measurement aligns with QED predictions, with an extraordinary precision of up to 12 decimal places

# $a_\ell$ measurements

## Electron

- One of the most precisely measured quantities in physics
- Measurement aligns with QED predictions, with an extraordinary precision of up to 12 decimal places

## Muon

- Precision up to 9 decimal places
- Persistent discrepancy between experimental measurements and theoretical predictions

# $a_\ell$ measurements

## Electron

- One of the most precisely measured quantities in physics
- Measurement aligns with QED predictions, with an extraordinary precision of up to 12 decimal places

## Muon

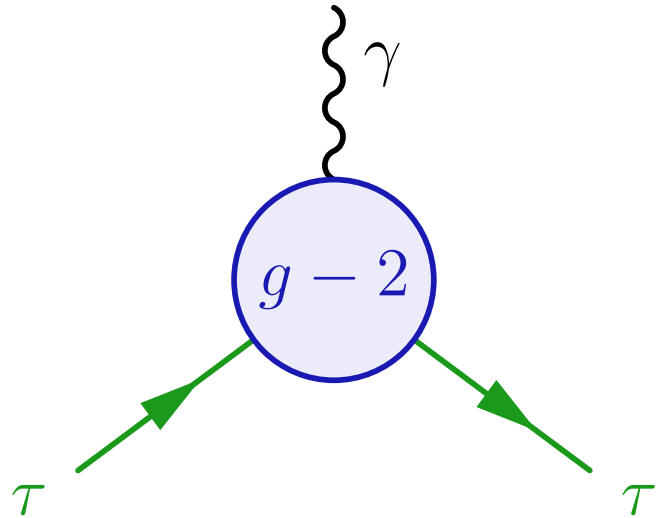
- Precision up to 9 decimal places
- Persistent discrepancy between experimental measurements and theoretical predictions

## Tau

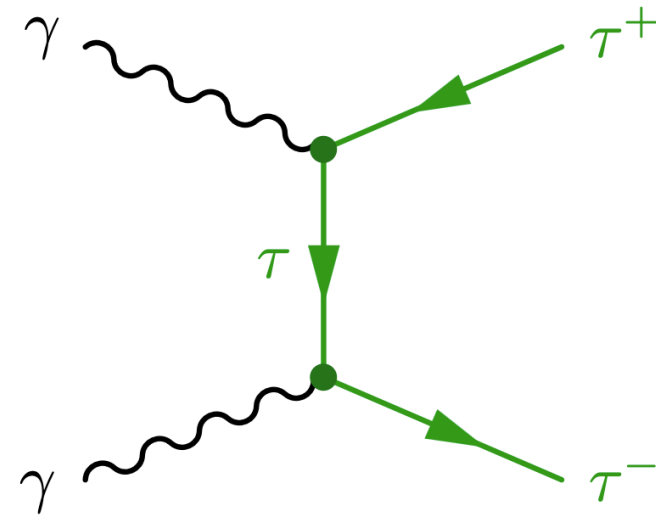
- Poorly measured because of short lifetime
- Limit from PDG dates back 20 years (LEP) and is about 20 times the Schwinger term
- If BSM effects scale with the  $m_\ell^2$ , deviations from SM could be 280 times larger than for  $a_\mu$

# $\tau$ electromagnetic moments from $\gamma\gamma \rightarrow \tau\tau$ events

- $\tau$   $g-2$  ( $a_\tau$ ) and electric dipole moment (EDM,  $d_\tau$ ) can be probed from  $\gamma\tau\tau$  vertex



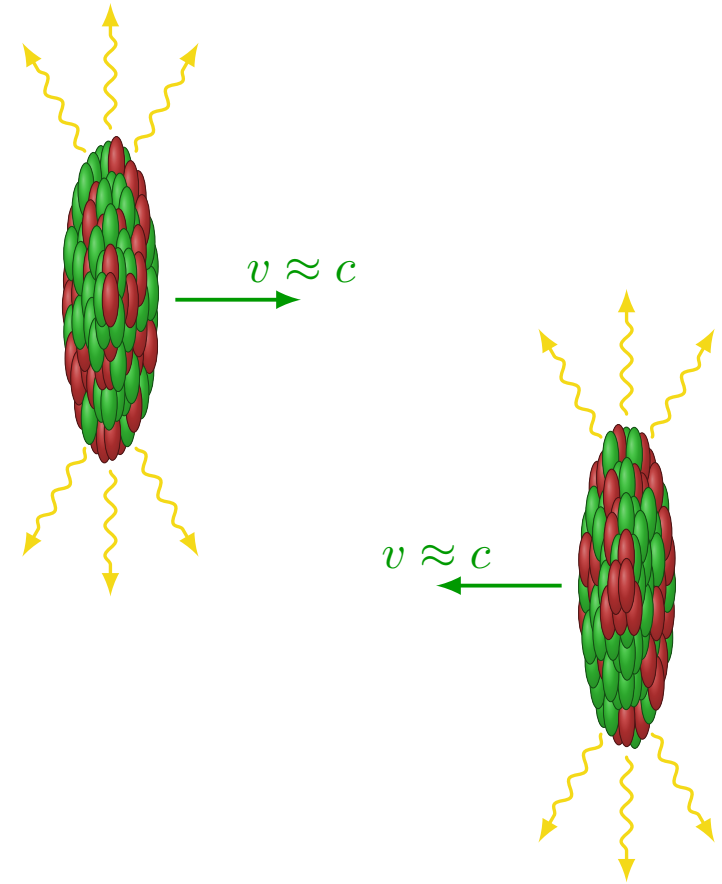
- The  $\gamma\gamma \rightarrow \tau\tau$  process includes 2  $\gamma\tau\tau$  vertices



- Constraints on  $\tau$  electromagnetic moments from form factor formalism or SMEFT approach
- In the SM,  $d_\tau$  is extremely small (no appreciable CP violation) but it could be increased in BSM models

# Photon-induced processes

- As two charged particles (e.g. protons or ions) pass each other at relativistic velocities, they generate intense electromagnetic fields → **photon-photon collisions** can happen

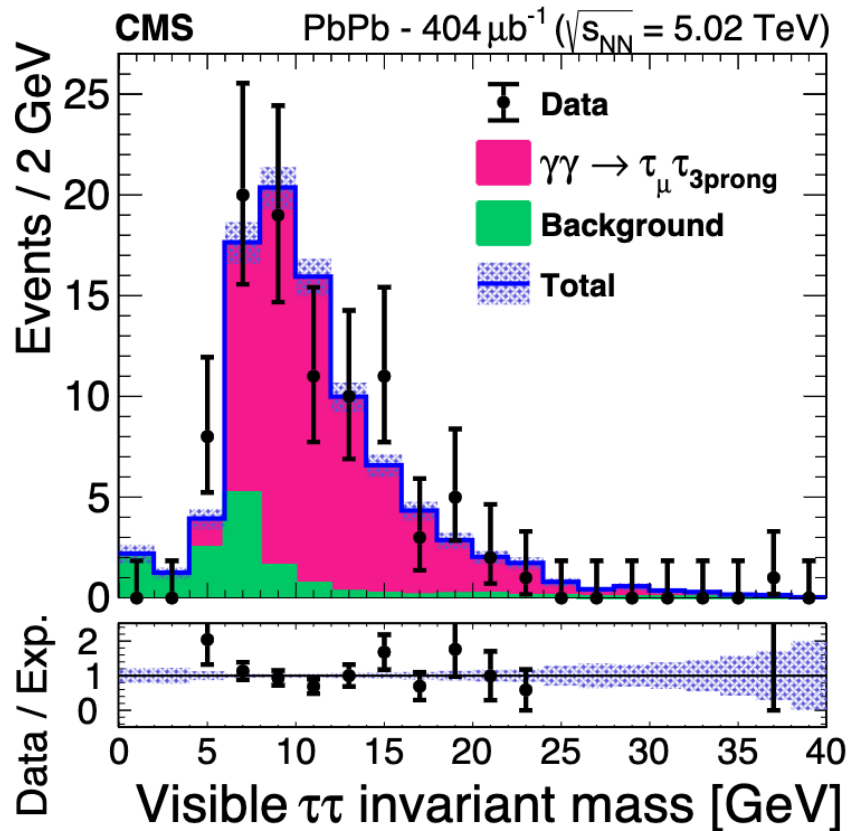


- **Cross section proportional to  $Z^4$**  → huge enhancement in Pb-Pb runs compared to pp runs

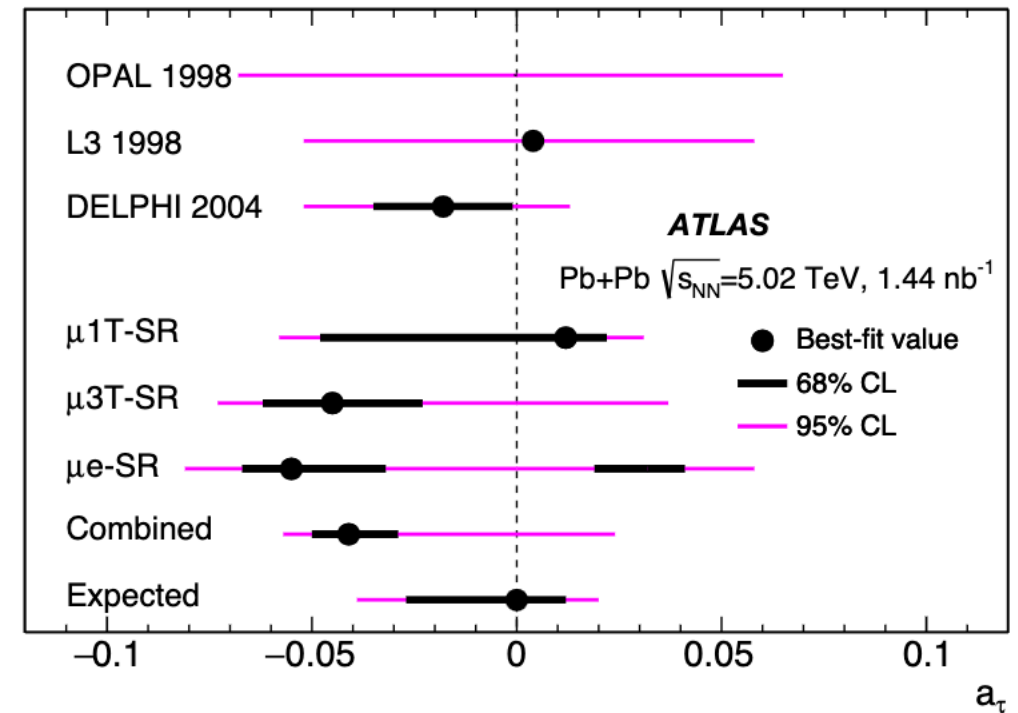


# $\gamma\gamma \rightarrow \tau\tau$ in Pb-Pb ultraperipheral collisions

- $\gamma\gamma \rightarrow \tau\tau$  observed recently in Pb-Pb collisions by both [CMS](#) and [ATLAS](#)



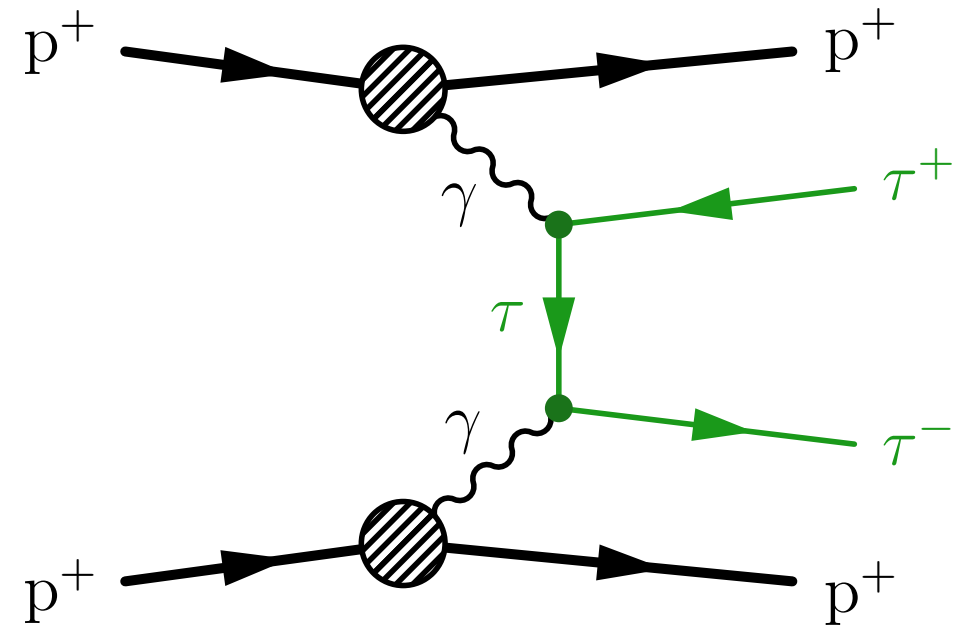
- Clean channel with small background contributions
- Accessing phase space with  $m_{\tau\tau} \gtrsim 25 \text{ GeV}$



Used to set constraints on  $a_{\tau}$ , close to best result from DELPHI

# Can we see $\gamma\gamma \rightarrow \tau\tau$ in ultraperipheral pp collisions?

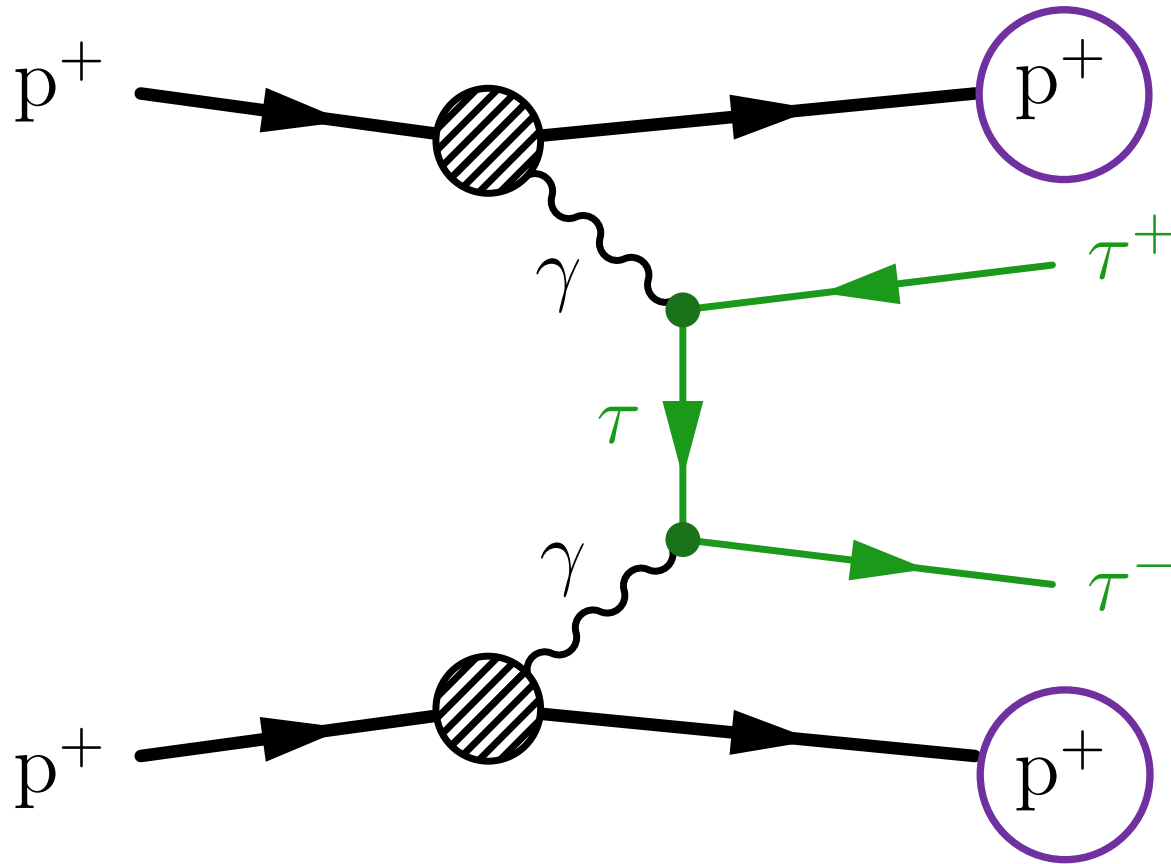
- Much larger integrated luminosity ( $O(10^8)$ )
- But:
  - No gain from  $Z^4$  enhancement
  - Low signal acceptance (soft signal)
  - Large backgrounds
  - High pileup



- If we can see  $\gamma\gamma \rightarrow \tau\tau$  in pp runs, tight constraints on  $\tau$  g-2 could be set because  **$a_\tau$  modifications from BSM physics are enhanced at large  $\tau$   $p_\tau$  and ditau mass**

# Signature

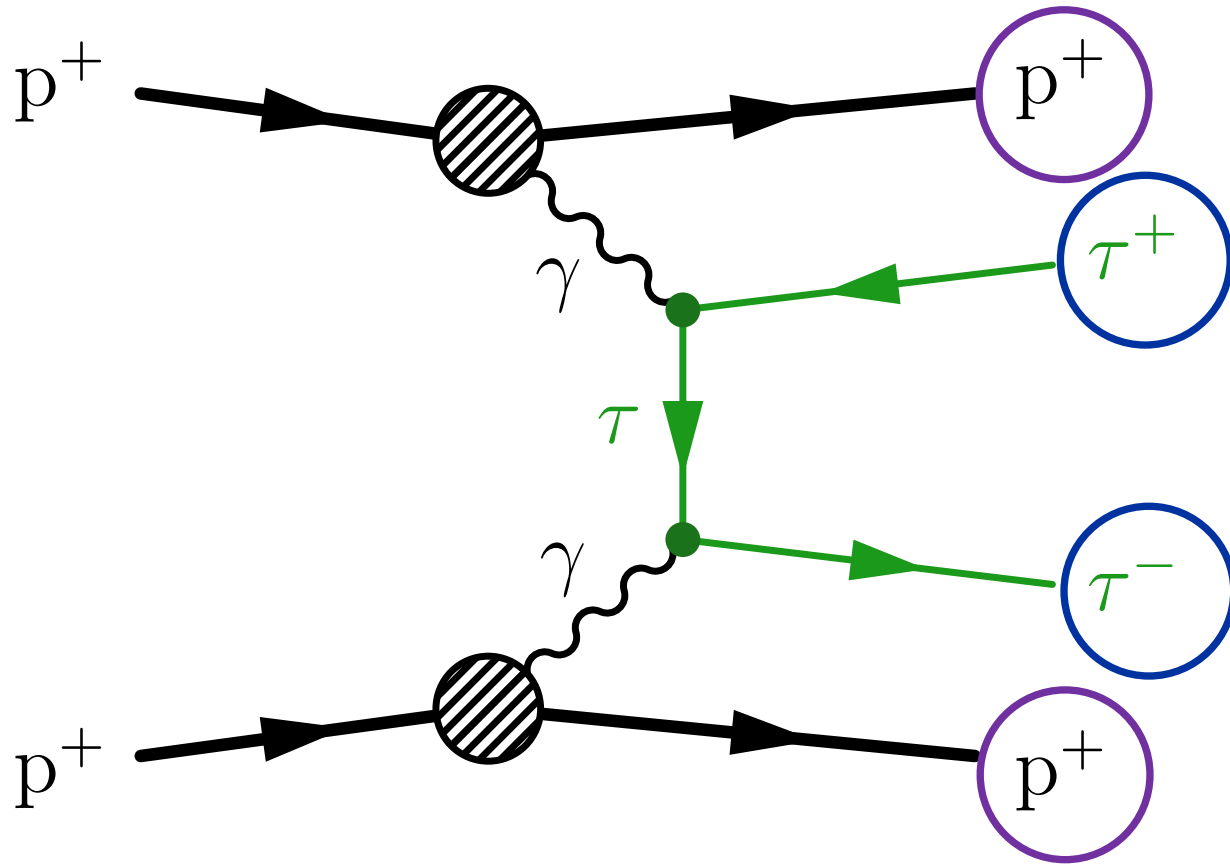
# Signature



- 2 diffracted protons
  - Could be reconstructed in PPS (Precision Proton Spectrometer) if  $m_{\tau\tau} \gtrsim 350 \text{ GeV} \rightarrow$  low signal acceptance
  - Decided not to require diffracted protons in the analysis

Elastic process, protons do not dissociate

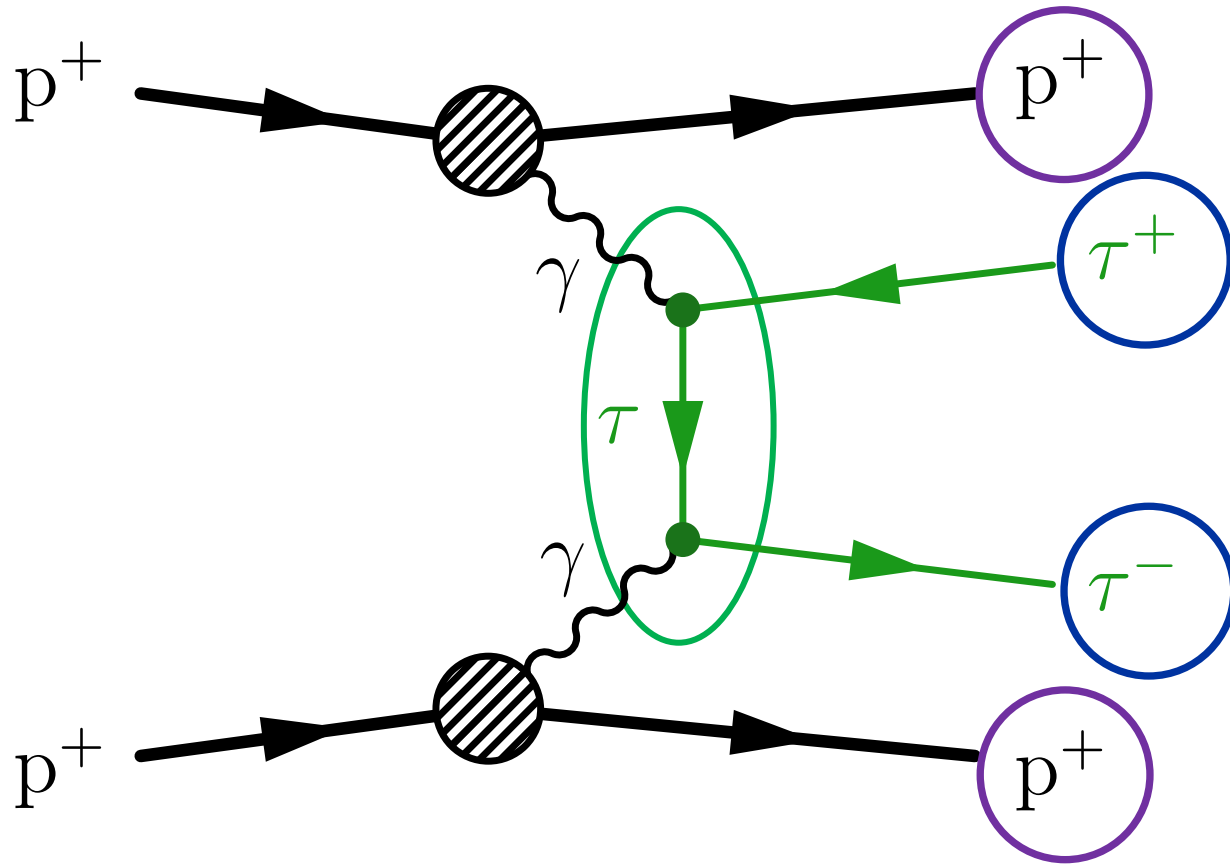
# Signature



- 2 diffracted protons
- 2 back-to-back OS  $\tau$  leptons
  - Acoplanarity  $A = 1 - \frac{|\Delta\phi|}{\pi} \approx 0$

Elastic process, protons do not dissociate

# Signature

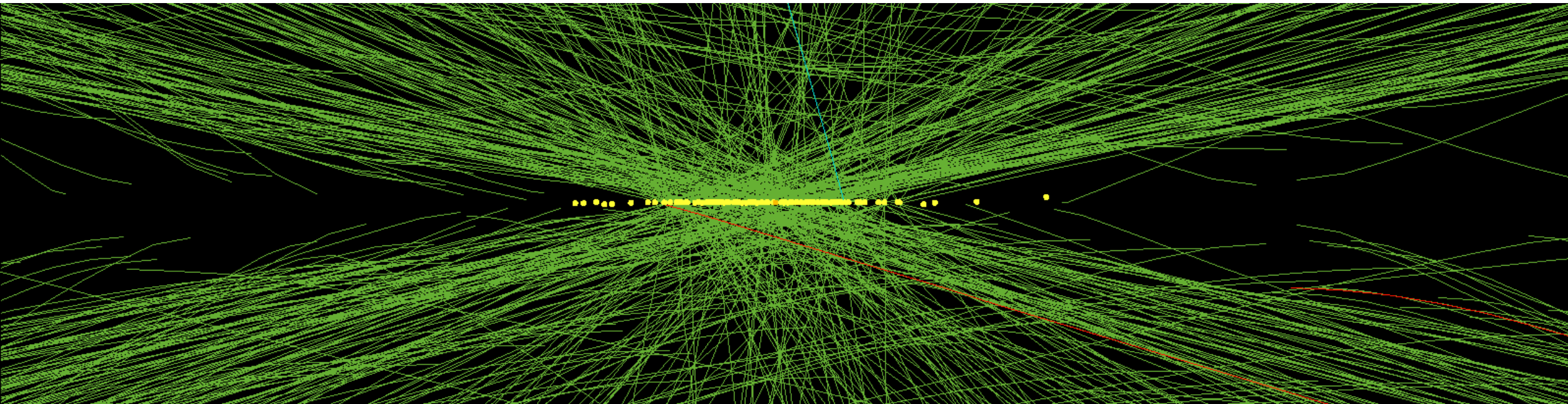


- 2 diffracted protons
- 2 back-to-back OS  $\tau$  leptons
- No hadronic activity close to the di- $\tau$  vertex
  - $N_{\text{tracks}} = 0$

Elastic process, protons do not dissociate

# Counting tracks

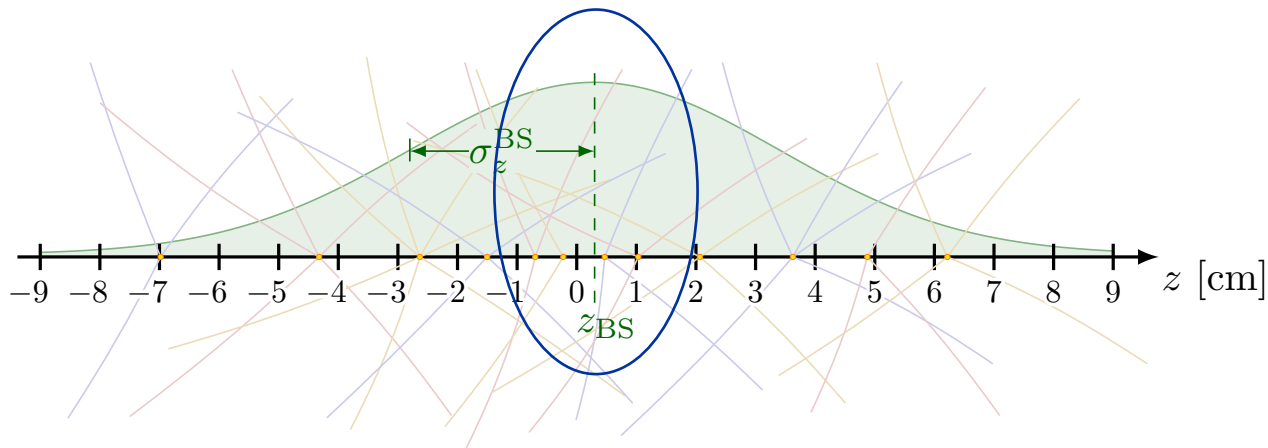
- Photon-induced processes are exceptionally clean...
- ... but proton-proton collisions are incredibly busy
  - Average of  $> 30$  pileup interactions in 2018



# Counting tracks

- Define **z position of di-tau vertex** as average z position of selected tau leptons
- Define  $N_{\text{tracks}}$  as the number of tracks
  - with  $p_{\text{T}} > 0.5$  GeV and  $|\eta| < 2.5$
  - within a window of **0.1 cm** around the di-tau vertex
  - Excluding tracks from tau leptons

*Extraordinary tracking capabilities  
of the CMS detector!*



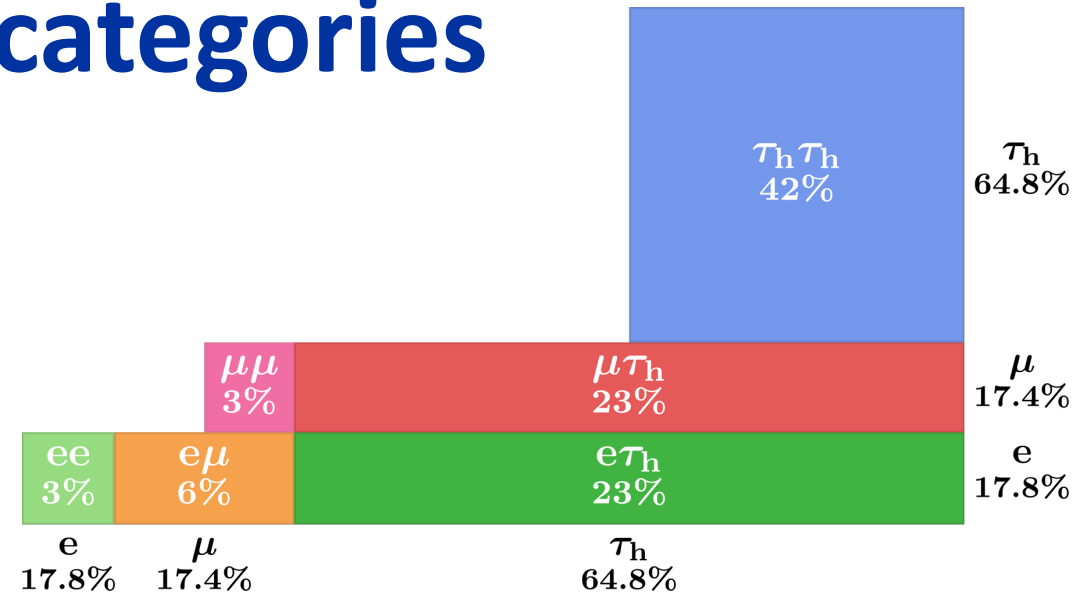
- About 30% of the windows at the center of the beamspot do not contain any pileup track



# Analysis overview

# Final states and categories

- 4 di-tau final states:  $e\mu$ ,  $e\tau_h$ ,  $\mu\tau_h$ ,  $\tau_h\tau_h$



- In each di-tau final state, 2 signal regions:  $N_{\text{tracks}} = 0$  or  $1$ 
  - $N_{\text{tracks}} = 0$ :  $\sim 50\%$  of the signal, inclusive backgrounds reduced by  $O(10^3)$
  - $N_{\text{tracks}} = 1$ :  $\sim 25\%$  of the signal, larger background
- Dimuon control region to derive corrections to the simulations

# Strategy

- In each of the 8 categories ( $e\mu$ ,  $e\tau_h$ ,  $\mu\tau_h$ ,  $\tau_h\tau_h$ )  $\times$  ( $N_{\text{tracks}} = 0$ ,  $N_{\text{tracks}} = 1$ ), fit visible invariant mass of tau pair ( $m_{\text{vis}}$ )
  - SM  $\gamma\gamma \rightarrow \tau\tau$  measurement: S/B ratio increases with  $m_{\text{vis}}$  because Drell-Yan background concentrated at lower masses
  - BSM  $a_\tau$  and  $d_\tau$  measurements: deviations from SM predictions increase with the mass

# Strategy

- In each of the 8 categories ( $e\mu, e\tau_h, \mu\tau_h, \tau_h\tau_h$ )  $\times$  ( $N_{\text{tracks}} = 0, N_{\text{tracks}} = 1$ ), fit visible invariant mass of tau pair ( $m_{\text{vis}}$ )
  - SM  $\gamma\gamma \rightarrow \tau\tau$  measurement: S/B ratio increases with  $m_{\text{vis}}$  because Drell-Yan background concentrated at lower masses
  - BSM  $a_\tau$  and  $d_\tau$  measurements: deviations from SM predictions increase with the mass

Drell-Yan  $Z/\gamma^* \rightarrow \tau\tau/ee/\mu\mu$

Resonant

From simulation

Jet  $\rightarrow e/\mu/\tau_h$  mis-ID

Non-resonant

From data

Exclusive  $\gamma\gamma \rightarrow ee/\mu\mu/WW$

Small but at low  $N_{\text{tracks}}$

From elastic simulation

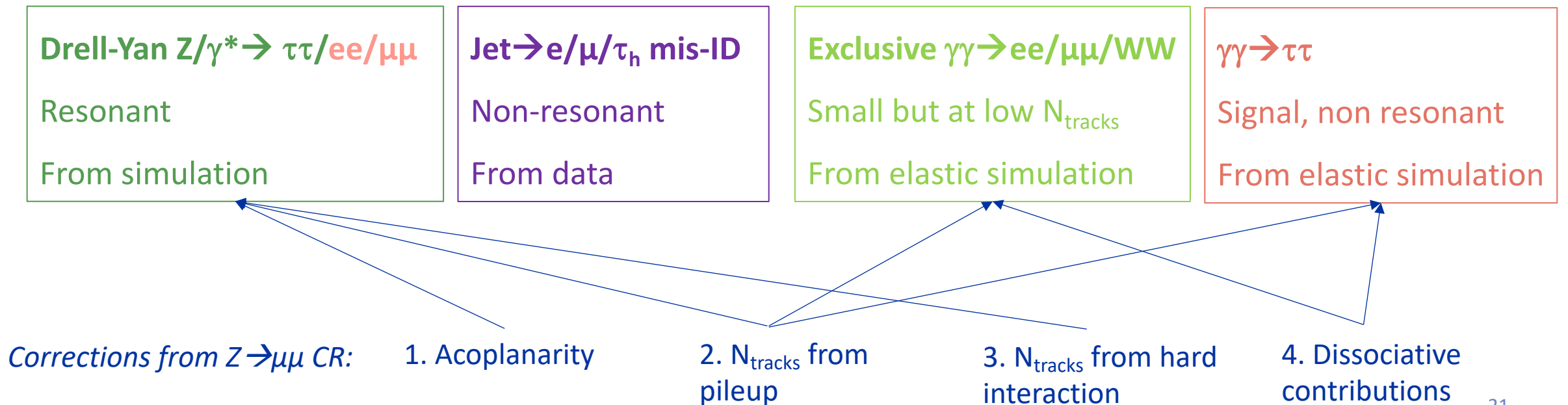
$\gamma\gamma \rightarrow \tau\tau$

Signal, non resonant

From elastic simulation

# Strategy

- In each of the 8 categories ( $e\mu, e\tau_h, \mu\tau_h, \tau_h\tau_h$ )  $\times$  ( $N_{\text{tracks}} = 0, N_{\text{tracks}} = 1$ ), fit visible invariant mass of tau pair ( $m_{\text{vis}}$ )
  - SM  $\gamma\gamma \rightarrow \tau\tau$  measurement: S/B ratio increases with  $m_{\text{vis}}$  because Drell-Yan background concentrated at lower masses
  - BSM  $a_\tau$  and  $d_\tau$  measurements: deviations from SM predictions increase with the mass



# Selection

Electron + muon triggers

Single lepton or lepton +  $\tau_h$  triggers  
 $p_T(\tau_h) > 30$  GeV to reduce fakes

	$e\mu$	$e\tau_h$	$\mu\tau_h$	$\tau_h\tau_h$	$\mu\mu$
$p_T^e$ (GeV)	$> 15/24$	$> 25 - 33$	—	—	—
$ \eta^e $	$< 2.5$	$< 2.1 - 2.5$	—	—	—
$p_T^\mu$ (GeV)	$> 24/15$	—	$> 21 - 29$	—	$> 26 - 29/10$
$ \eta^\mu $	$< 2.4$	—	$< 2.1 - 2.4$	—	—
$p_T^{\tau_h}$ (GeV)	—	$> 30 - 35$	$> 30 - 32$	$> 40$	—
$ \eta^{\tau_h} $	—	$< 2.1 - 2.3$	$< 2.1 - 2.3$	$< 2.1$	—
$m_{\mu\mu}$ (GeV)	—	—	—	—	$> 50$
OS	yes	yes	yes	yes	yes
$ d_z(\ell, \ell') $ (cm)	$< 0.1$	$< 0.1$	$< 0.1$	$< 0.1$	$< 0.1$
$\Delta R(\ell, \ell')$	$> 0.5$	$> 0.5$	$> 0.5$	$> 0.5$	$> 0.5$
$m_T(e/\mu, \vec{p}_T^{\text{miss}})$ (GeV)	—	$< 75$	$< 75$	—	—

Di-tau trigger

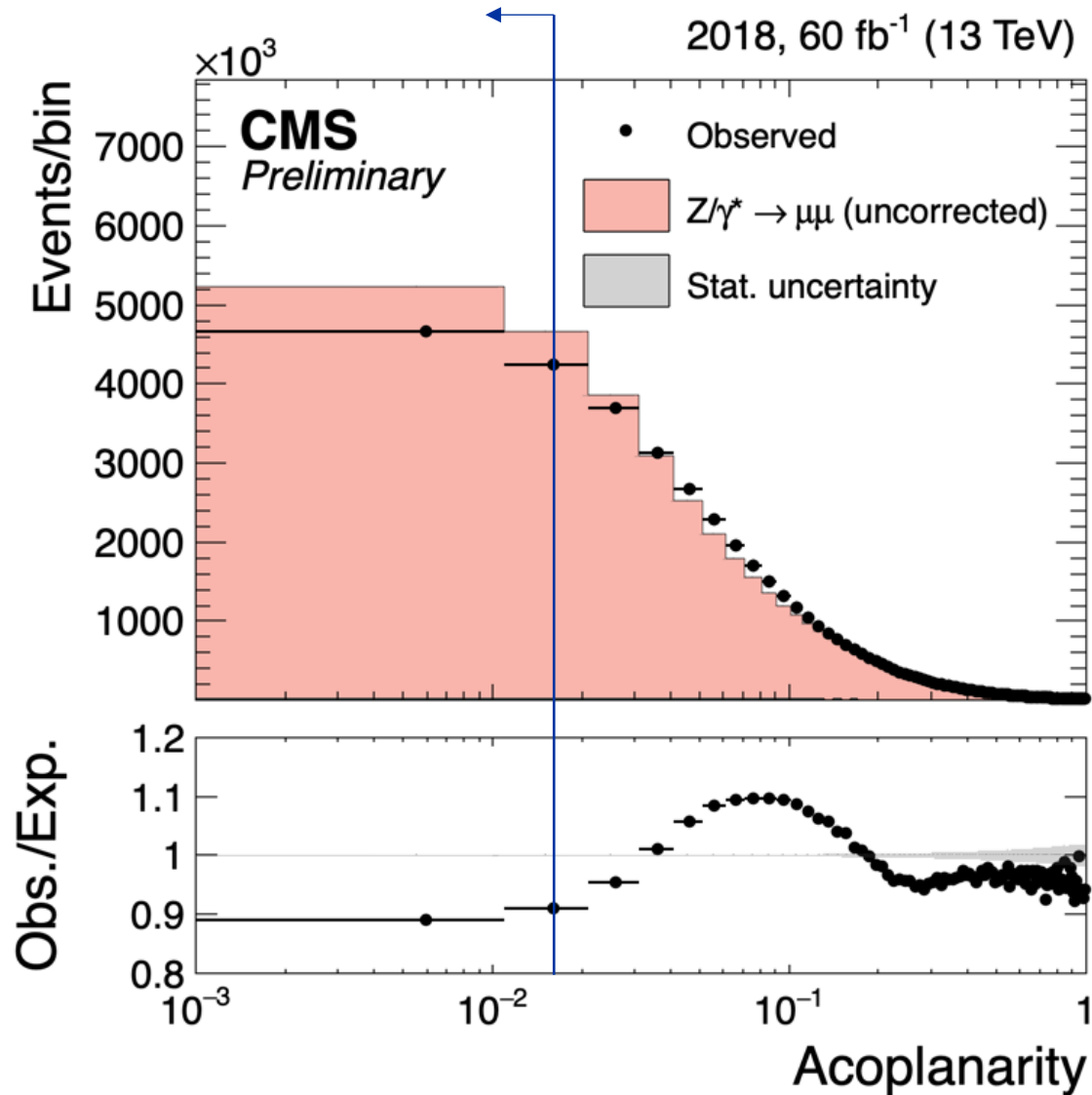
To reduce  
W+jets  
background

In the signal regions, also require  $\mathbf{A} = 1 - \frac{|\Delta\phi|}{\pi} < 0.015$  and  $N_{\text{tracks}} = 0$  or  $1$

**μμ control region – deriving  
corrections to the simulations**

# 1. Acoplanarity correction

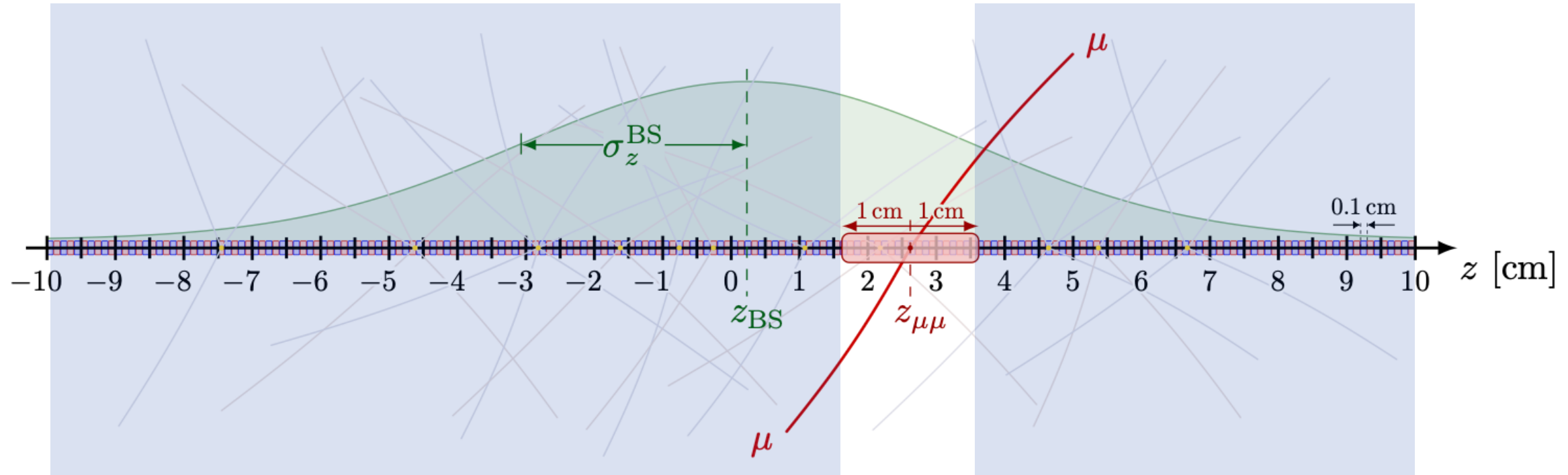
Signal region,  $A < 0.015$



- The Drell-Yan simulation (*aMC@NLO*, *FxFx merging*) does not model well the acoplanarity distribution in the dimuon control region
- The mismodeling depends on the lepton  $p_T$
- Derive corrections to acoplanarity distribution in 2D bins of leading and subleading lepton  $p_T$
- Corrects Z  $p_T$  distribution simultaneously

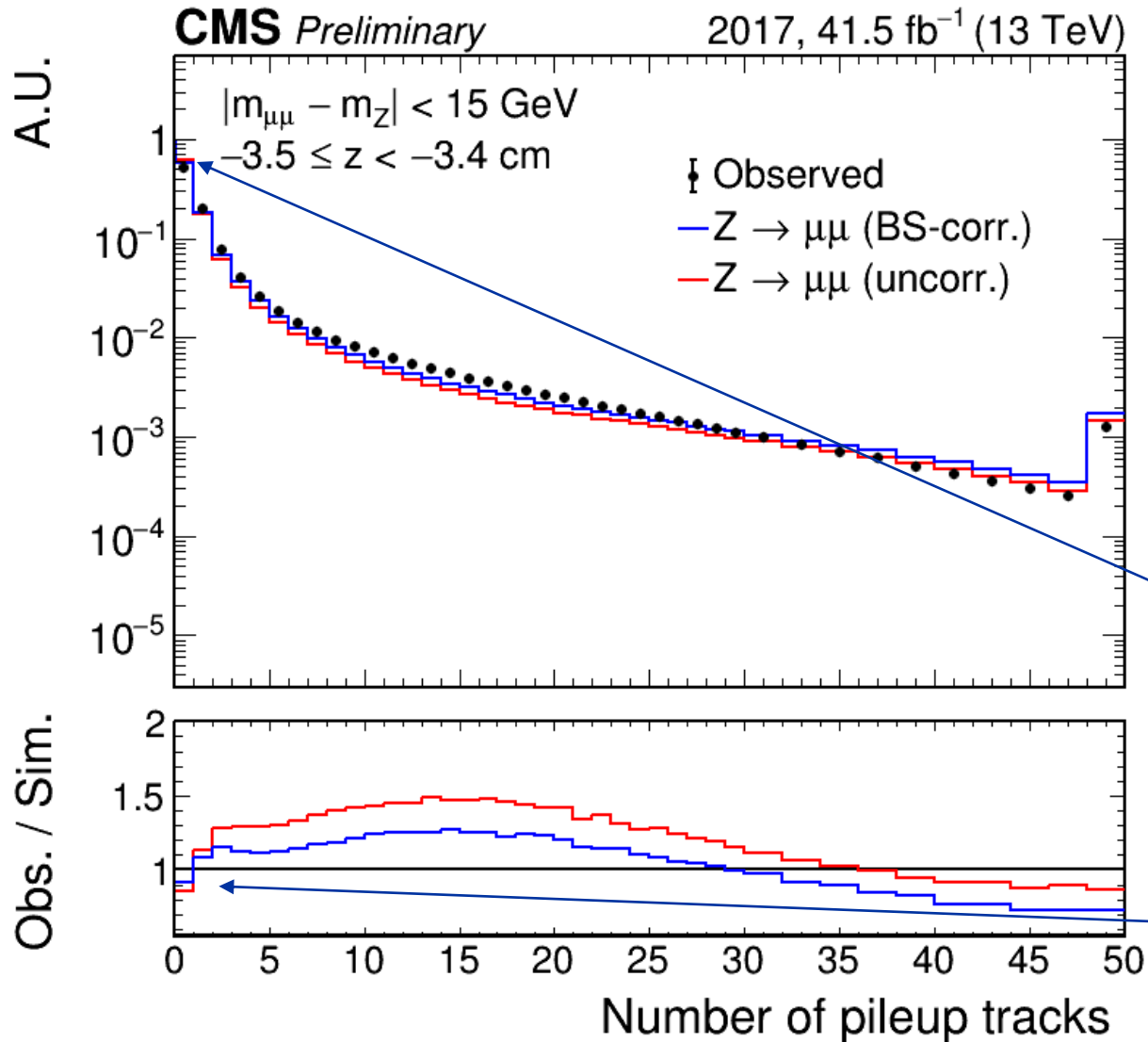


## 2. Pileup track multiplicity correction



- Can simulations describe accurately the number of pileup tracks within windows of 0.1 cm width all over the z axis?
- Compare  $N_{\text{tracks}}$  distribution in  $Z \rightarrow \mu\mu$  data and  $Z \rightarrow \mu\mu$  MC, inside **windows** sampled over the z axis far ( $> 1\text{cm}$ ) from the  $\mu\mu$  vertex

## 2. Pileup track multiplicity correction

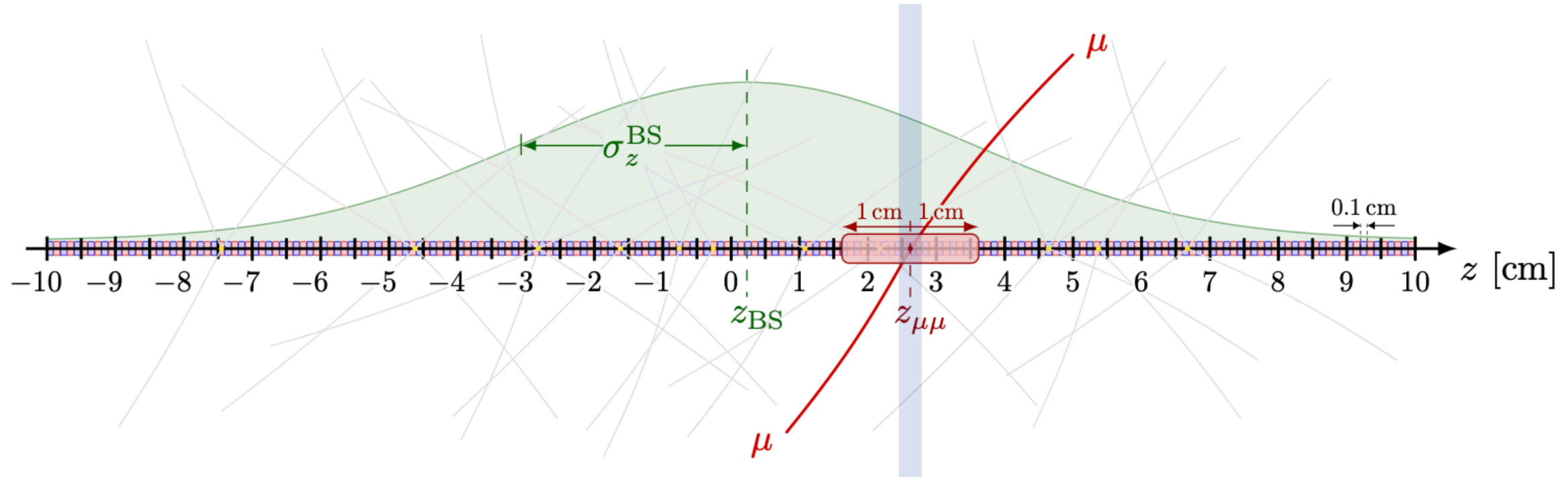


- First, correct simulated  $z$  position and width of beamspot (constant values) to match the profiles in data
- Then, derive event-weight correction as a function of  $N_{\text{tracks}}$  and  $z$

1 beamspot width away from beamspot center,  
 50% of windows do not contain any PU track

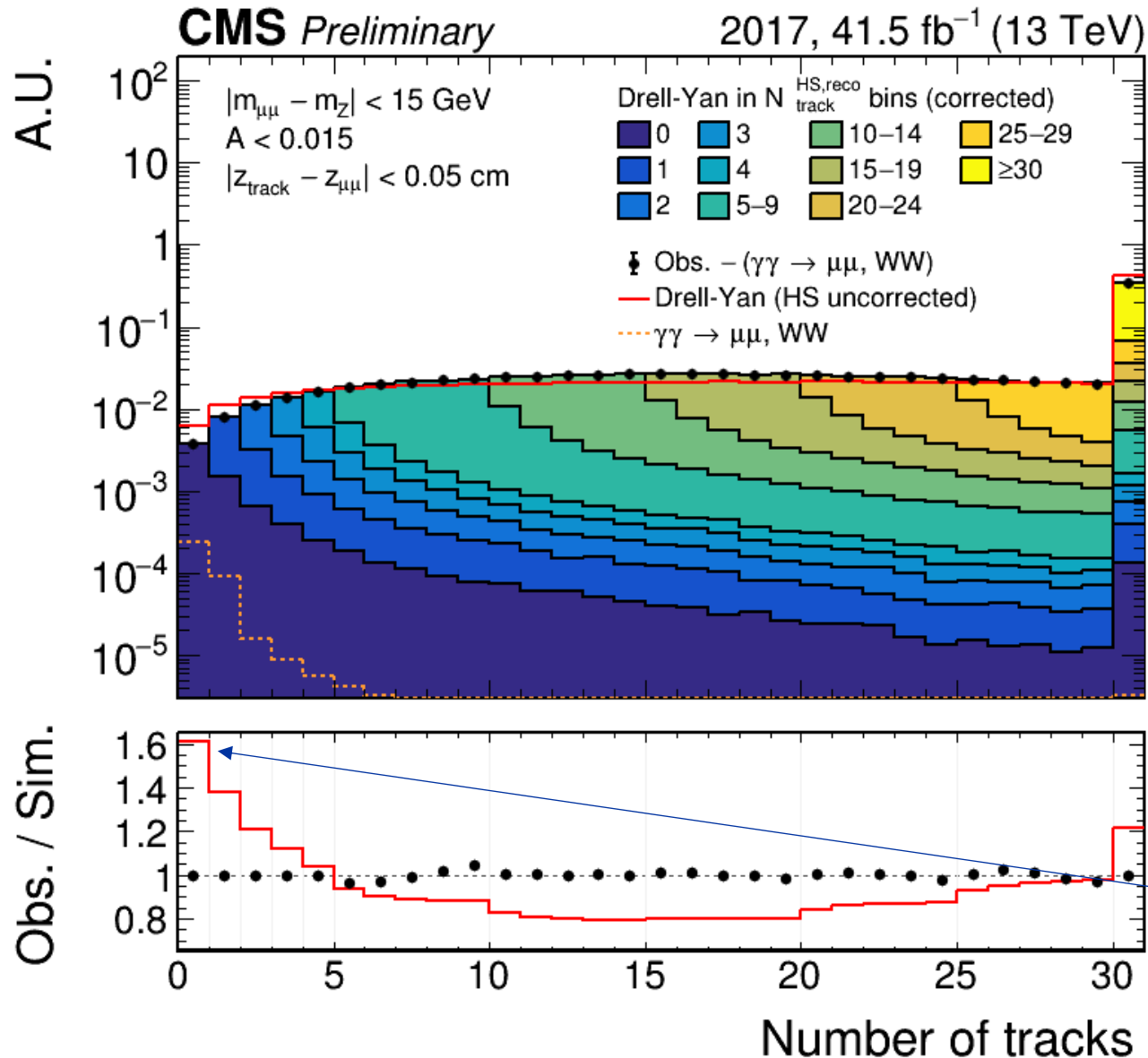
For a window 1 beamspot width away from  
 beamspot center with no PU track inside, the  
 event-weight correction is 0.95

# 3. Hard scattering track multiplicity correction



- Can the Drell-Yan simulation describe accurately the number of tracks from the hard interaction in windows of 0.1 cm width?
- Compare  $N_{\text{tracks}}$  distribution in  $Z \rightarrow \mu\mu$  data and  $Z \rightarrow \mu\mu$  MC (subtracting elastic processes), inside window centered at the  $\mu\mu$  vertex

# 3. Hard scattering track multiplicity correction

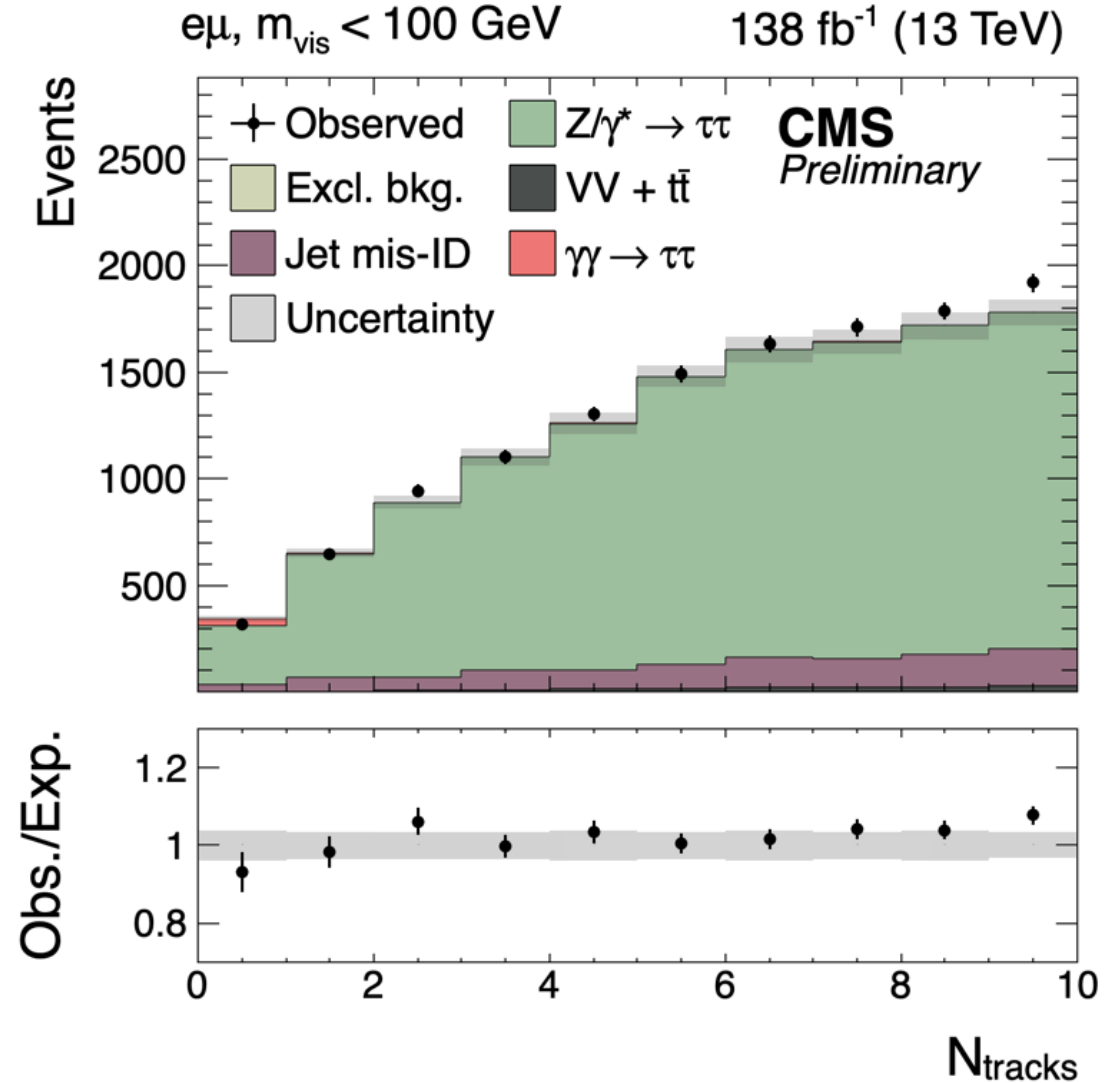


- Compare number of reconstructed tracks in data and in DY simulation at the  $\mu\mu$  vertex
- These tracks can come from pileup or from the hard interaction
- Split simulation based on the number of reconstructed tracks associated to the hard interaction, and rescale all components simultaneously to match the data

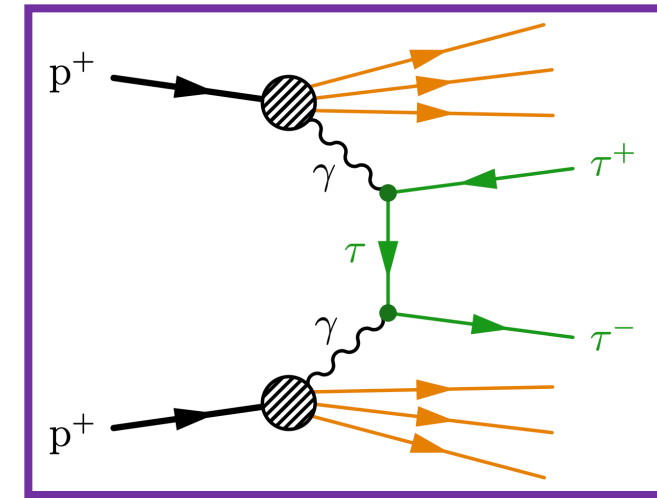
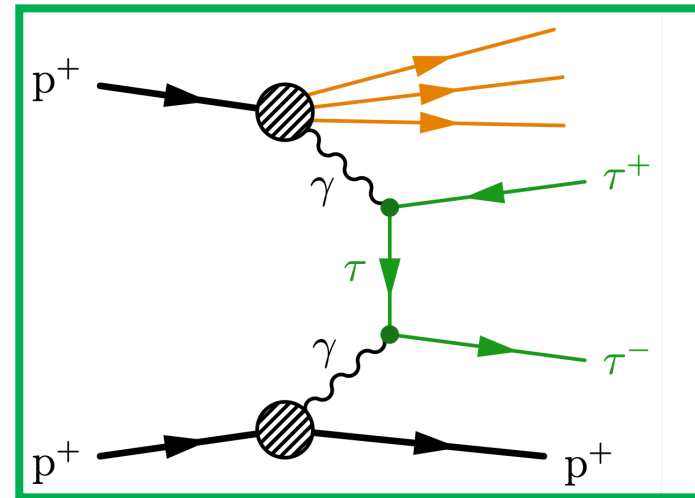
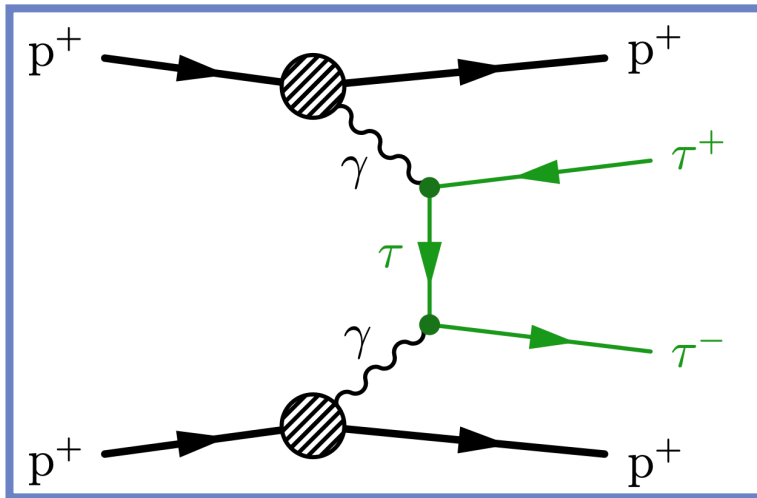
Simulated Drell-Yan events with no reconstructed track associated to the hard interaction in the  $\mu\mu$  window should be assigned a weight of  $1/1.6 = 0.625$

# Applying these corrections to $Z/\gamma^* \rightarrow \tau\tau$ simulation

- Good data/MC agreement in  $N_{\text{tracks}}$  distribution in all di-tau final states for the **DY-enriched** region with  $m_{\text{vis}}(\tau, \tau) < 100 \text{ GeV}$



# 4. Including (semi-)dissociative contributions



- **Elastic-elastic (ee)** signal process modeled with gammaUPC
- **Single-dissociative (sd)** and **double-dissociative (dd)** processes have larger cross section and may end up with an exclusive signature  $\rightarrow$  rescale elastic signal to include these contributions
- Scaling factor =  $(ee + sd + dd)_{obs} / ee_{sim}$  can be measured with  $\gamma\gamma \rightarrow \mu\mu$  in the  $\mu\mu$  CR and applied to  $\gamma\gamma \rightarrow ee/\mu\mu/\tau\tau/WW$  in the signal region

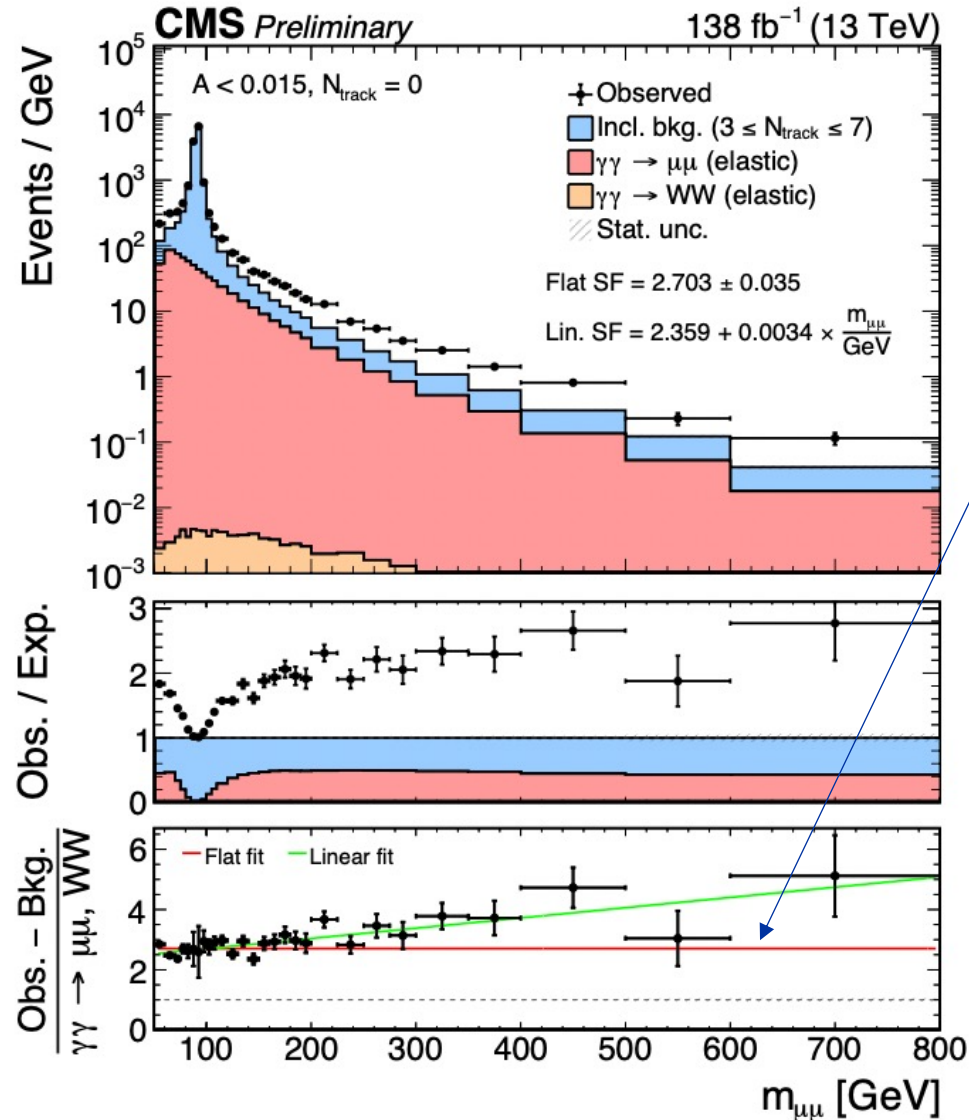
# 4. Including (semi-)dissociative contributions

- Inclusive backgrounds:**

- Shape from data with  $2 < N_{\text{tracks}} < 8$   
 → Negligible exclusive contributions
- Normalized to Z peak in events with  $N_{\text{tracks}} = 0$  or 1

- Elastic  $\gamma\gamma \rightarrow \mu\mu$ /WW:**

- Estimated from gammaUPC
- Rescaled with **linear  $m_{\mu\mu}$  function** to match data



*Elastic simulation should be scaled by ~2.7 to describe all photon-induced contributions*

*Compatible with SuperChic predictions*

# Jet mis-ID background modeling

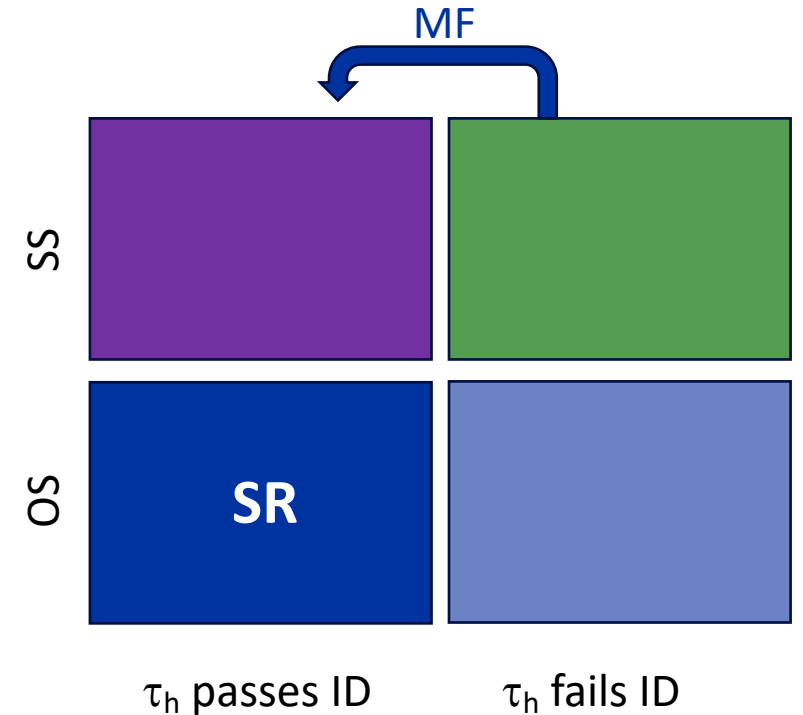


# Jet $\rightarrow \tau_h$ mis-ID background (1)

*$e \tau_h, \mu \tau_h, \tau_h \tau_h$  final states*

- Measure "mis-ID factor", MF, for jets as

$$MF = \frac{N(\text{jets passing nominal } \tau_h \text{ ID})}{N(\text{jets failing nominal } \tau_h \text{ ID but passing very loose } \tau_h \text{ ID})}$$



- As a function of the  $\tau_h$   $p_T$  and decay mode
- In data control regions (e.g. require SS leptons/ $\tau_h$  to enrich in QCD multijet events)

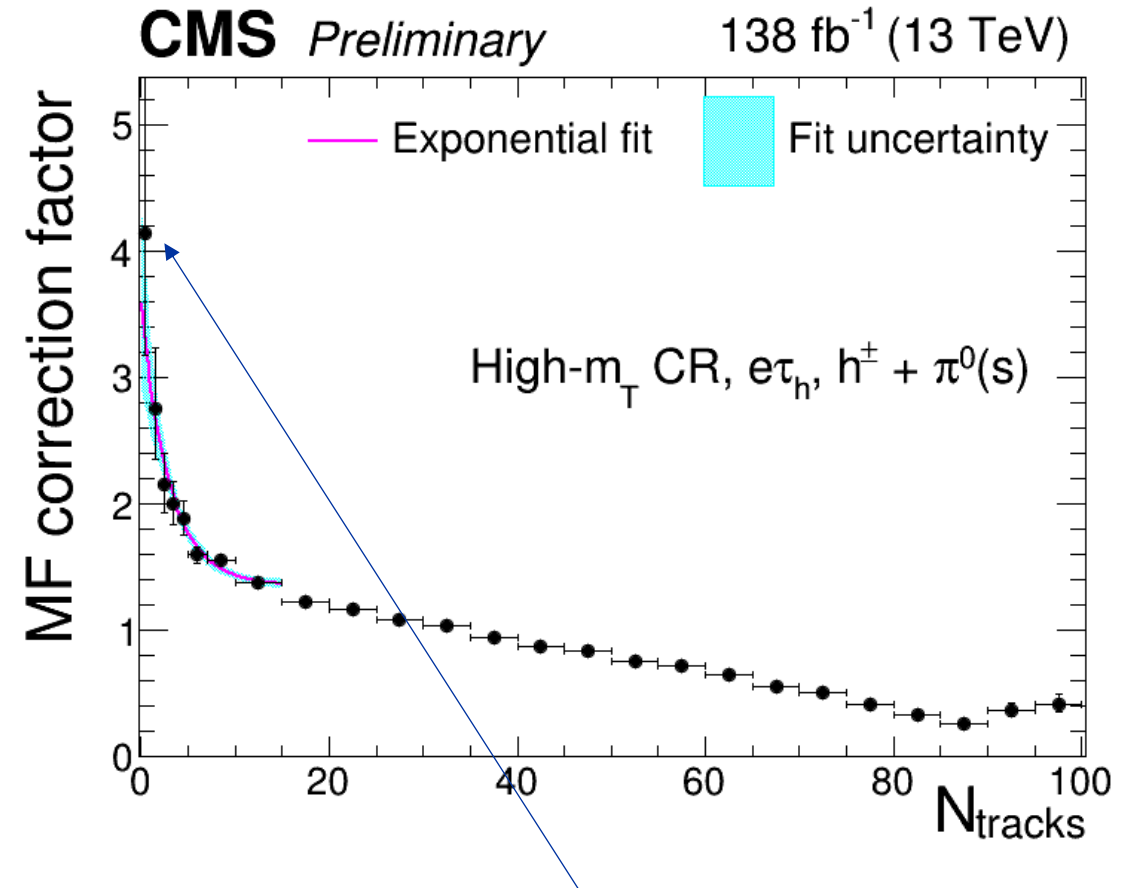
- To estimate background in the SR, select events passing the SR selection except the  $\tau_h$  fails the nominal  $\tau_h$  ID and reweigh them with MF

*But it is not that simple...*

*How does  $N_{tracks}$  affect MF?*

# Jet $\rightarrow \tau_h$ mis-ID background (2)

- If there is less track activity around the  $\tau_h$  candidate:
  - The  $\tau_h$  candidate is more isolated
  - It is more likely to pass the ID criteria
  - MF is higher
- Model  $N_{\text{tracks}}$  dependence with a multiplicative correction to the mis-ID rates
  - Parameterized with exponential at low  $N_{\text{tracks}}$

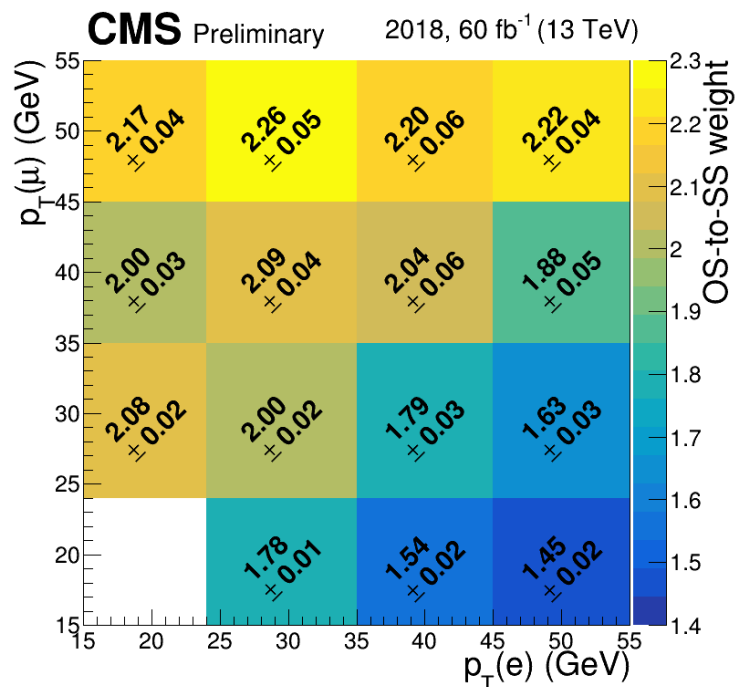


*The jet is 4 times more likely to pass the nominal  $\tau_h$  ID criteria if there is no other track at the vertex*

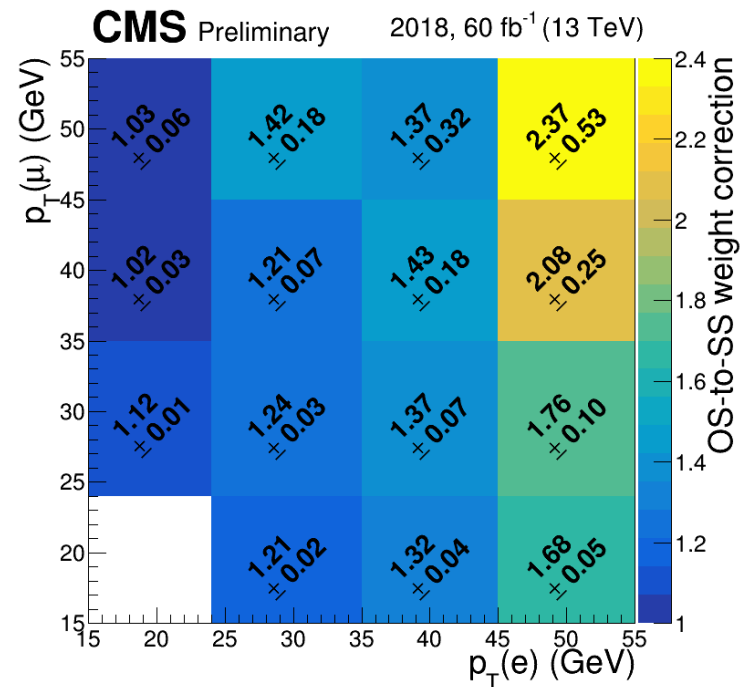
# Jet $\rightarrow$ e/μ background

- Normalization: reweigh SS events with SF made of 3 multiplicative terms
- Shape: SS events with  $N_{\text{tracks}} < 10$  to improve statistical precision

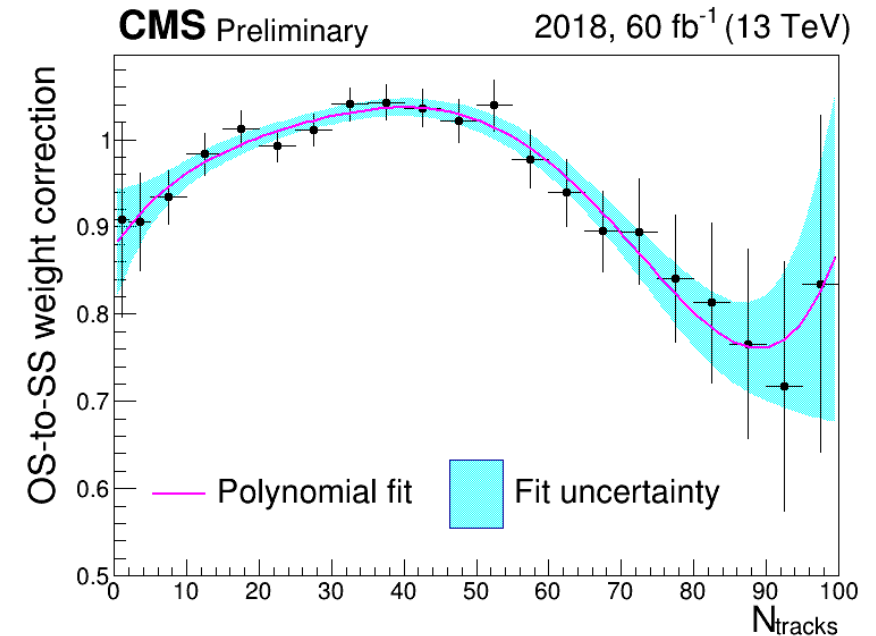
1. OS/SS SF measured in events with anti-isolated muon
2. Correction for muon inverted isolation
3.  $N_{\text{tracks}}$  corrections



1.



2.



3.

Observation of  $\gamma\gamma \rightarrow \tau\tau$

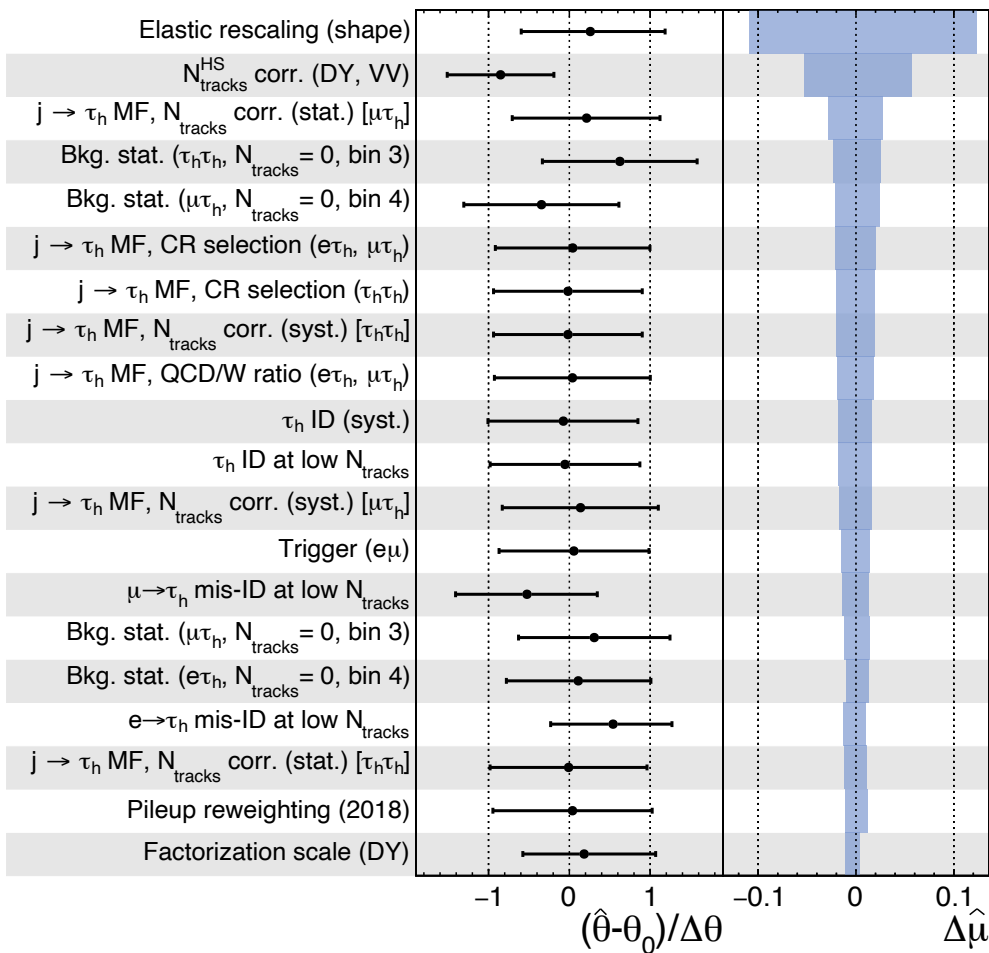
# Leading systematics

CMS Preliminary

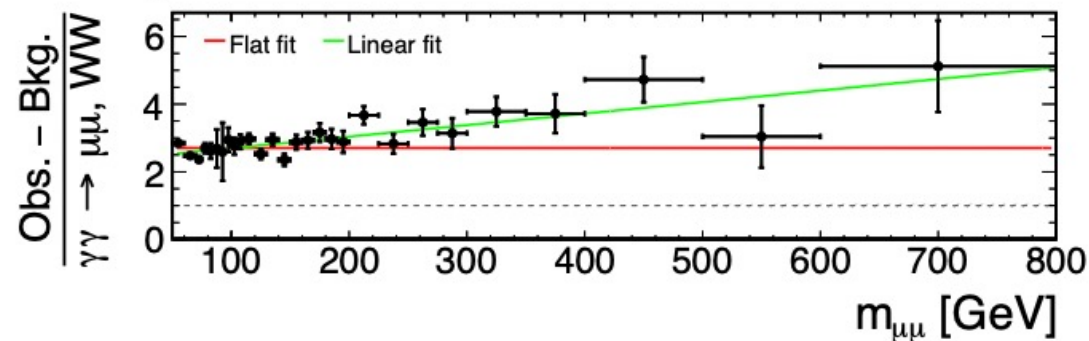
138 fb<sup>-1</sup> (13 TeV)

→ Fit   ±1 σ impact

$\hat{\mu} = 0.75^{+0.20}_{-0.18}$



Considering the constant rescaling for the elastic simulations instead of the  $m_{\mu\mu}$ -dependent one

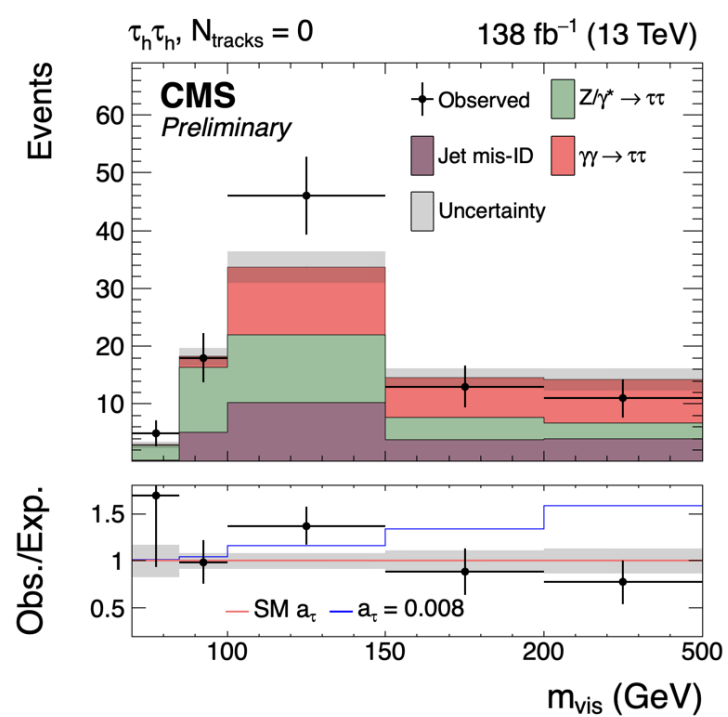
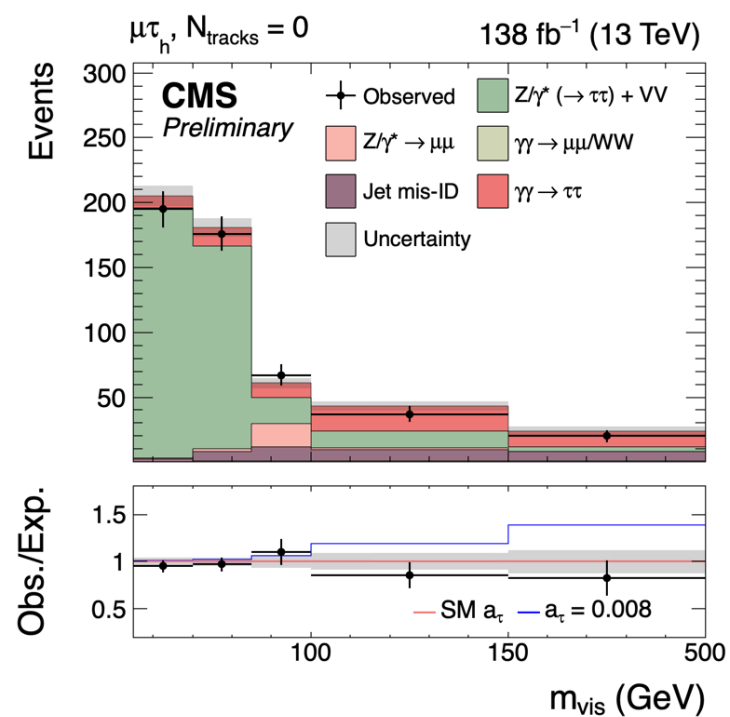
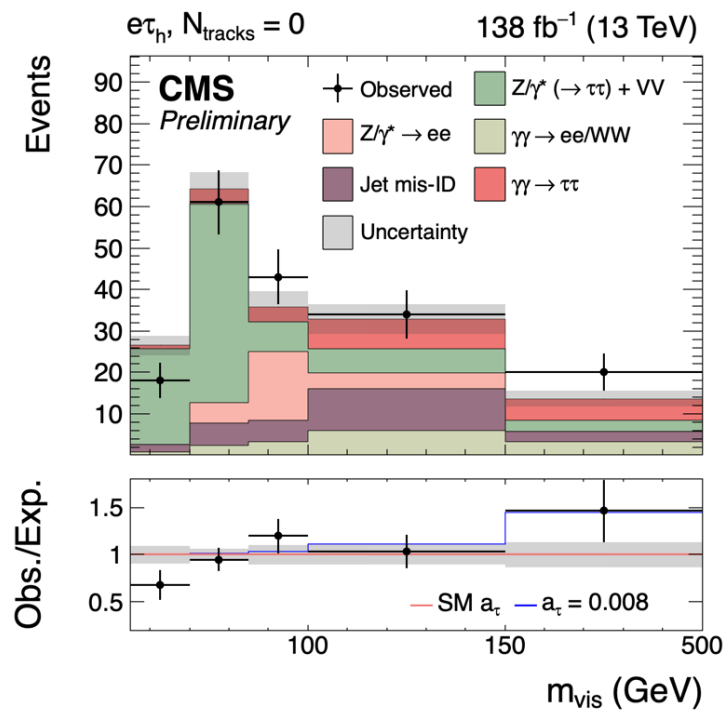
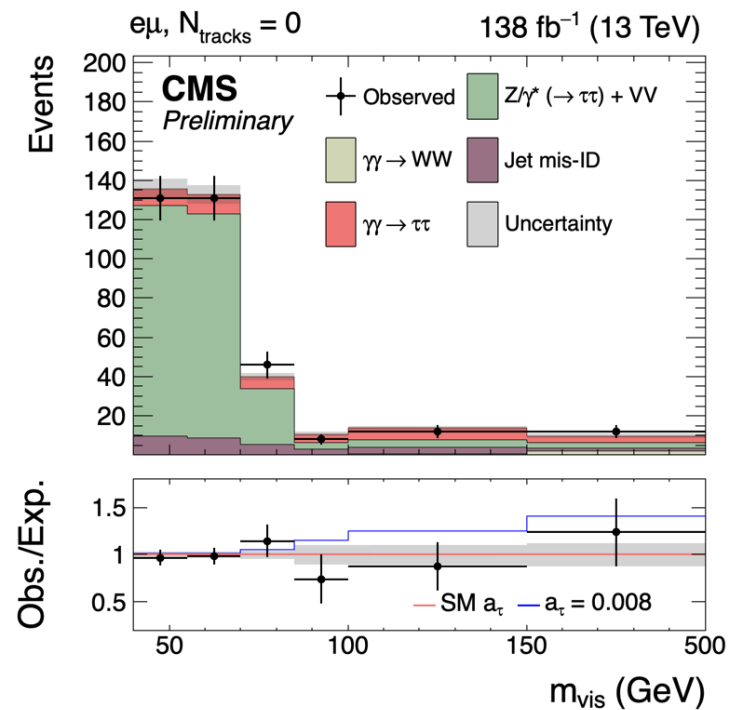


UE/HS track multiplicity correction to Drell-Yan (6.5% uncertainty for  $N_{\text{tracks}} = 0$ )

$N_{\text{tracks}}$  extrapolation of the jet  $\rightarrow \tau_h$  MF to estimate jet mis-ID background (up to ~20%)

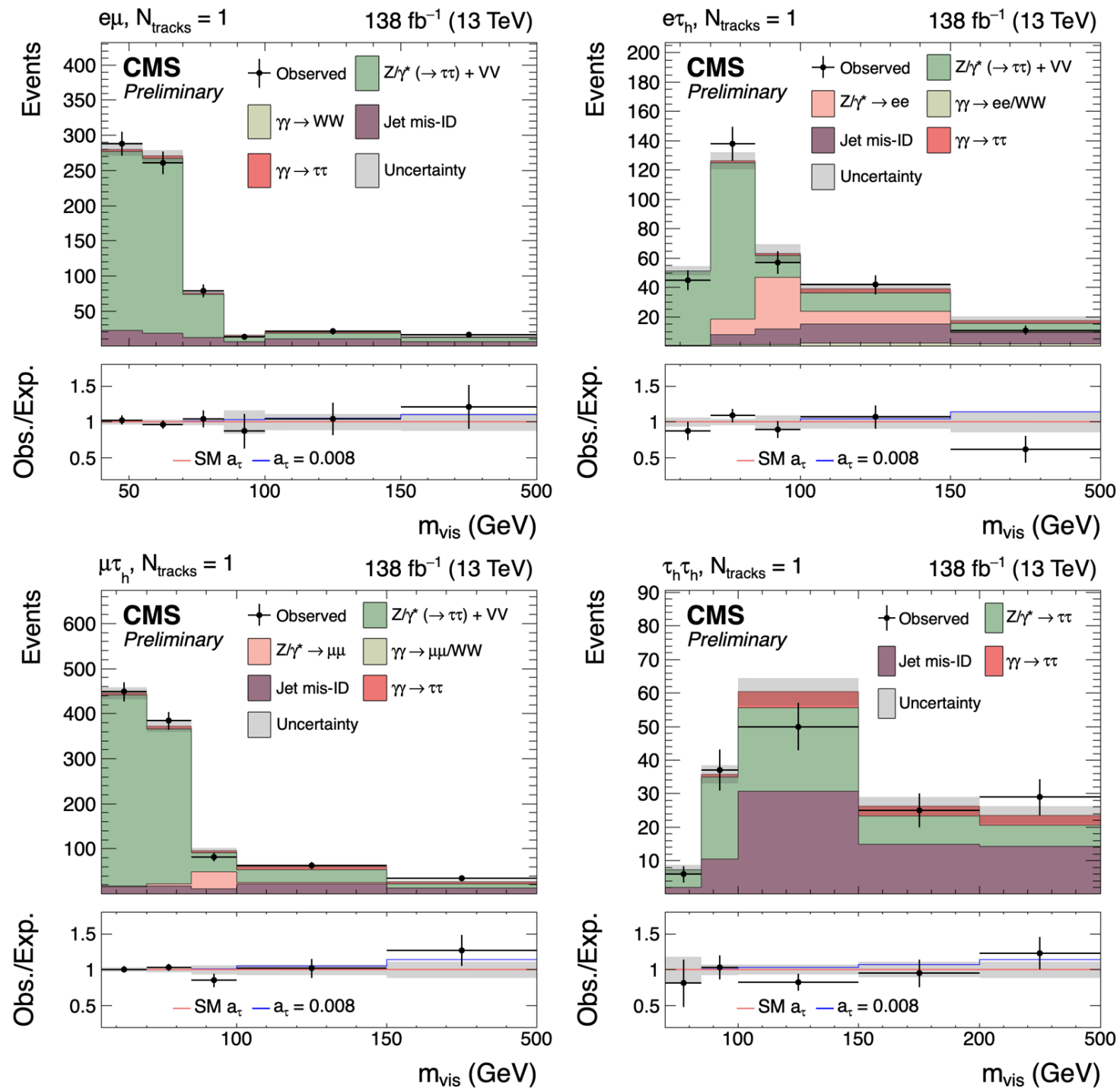
Real and fake  $\tau_h$  identification (at low  $N_{\text{tracks}}$ )

# $N_{\text{tracks}} = 0$



- $m_{\text{vis}}$  distributions in the different final states after the maximum likelihood fit, assuming SM  $a_\tau$  and  $d_\tau$
- **Signal visible in high  $m_{\text{vis}}$  bins**

# $N_{\text{tracks}} = 1$

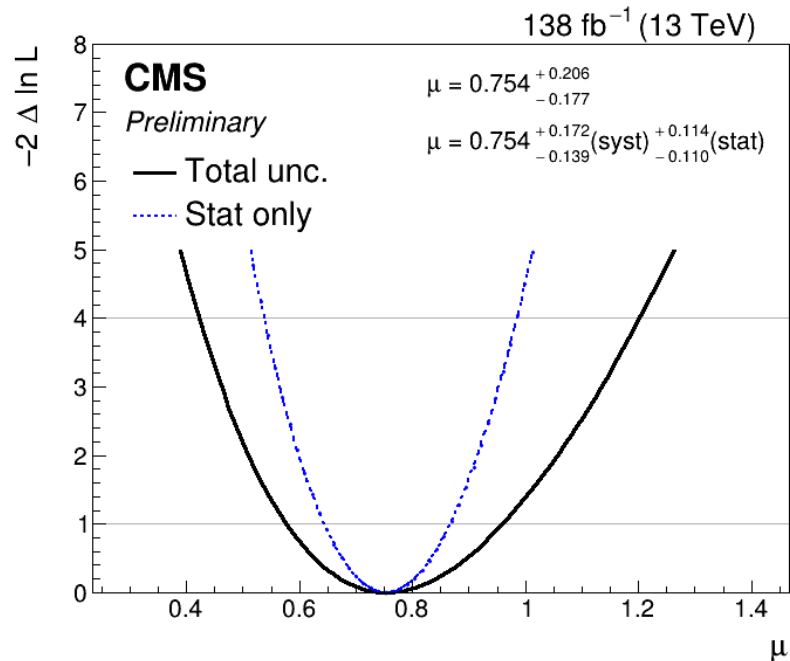


- $m_{\text{vis}}$  distributions in the different final states after the maximum likelihood fit, assuming SM  $a_\tau$  and  $d_\tau$
- Lower signal contributions and larger background  $\rightarrow$  validation of background modeling and adding some sensitivity

# Observation of $\gamma\gamma \rightarrow \tau\tau$

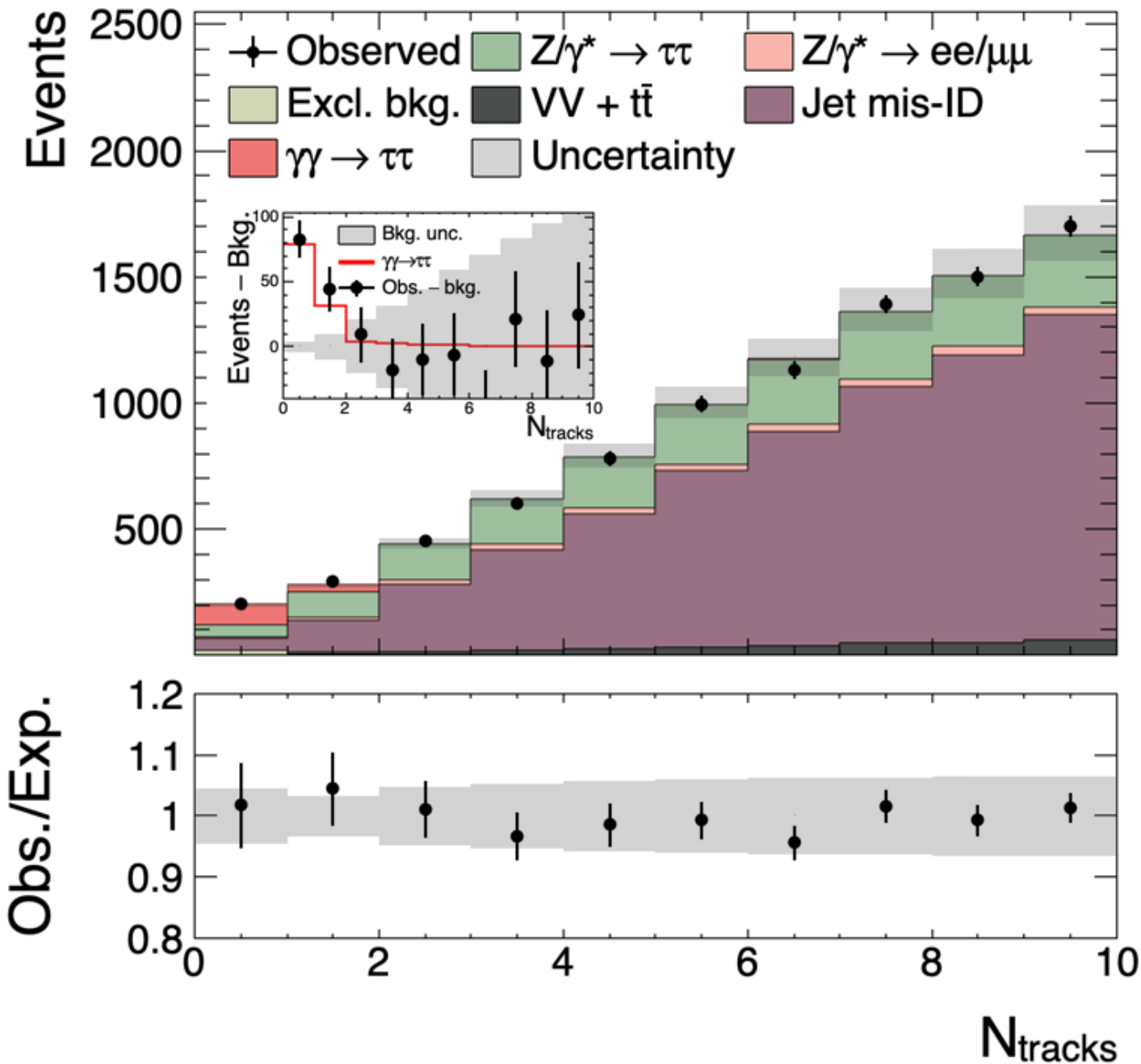
- 5.3  $\sigma$  observed, 6.5  $\sigma$  expected
- First observation of  $\gamma\gamma \rightarrow \tau\tau$  in pp runs

*Signal strength with respect to gammaUPC elastic prediction rescaled by our data-driven correction*



	Observed	Expected
$e\mu$	2.3 $\sigma$	3.2 $\sigma$
$e\tau_h$	3.0 $\sigma$	2.1 $\sigma$
$\mu\tau_h$	2.1 $\sigma$	3.9 $\sigma$
$\tau_h\tau_h$	3.4 $\sigma$	3.9 $\sigma$
Combined	5.3 $\sigma$	6.5 $\sigma$





- Postfit  $N_{\text{tracks}}$  distribution for  $m_{\text{vis}} > 100$  GeV

- We can model well the  $N_{\text{tracks}}$  distribution for backgrounds

- The signal is seen as an excess of events at very low  $N_{\text{tracks}}$

# Constraints on tau anomalous electromagnetic moments

# Constraining $a_\tau$ and $d_\tau$ with an EFT

- Two dimension-6 operators modify  $a_\tau$  and  $d_\tau$  at tree-level in the SMEFT:

$$\mathcal{L}_{\text{BSM}} = \frac{C_{\tau B}}{\Lambda^2} \bar{L}_L \sigma^{\mu\nu} \tau_R H B_{\mu\nu} + \frac{C_{\tau W}}{\Lambda^2} \bar{L}_L \sigma^{\mu\nu} \tau_R \sigma^i H W_{\mu\nu}^i + \text{h.c.}$$

- BSM contributions to  $a_\tau$  and  $d_\tau$ :

*SMEFT-sim\_general alphaScheme\_UFO*

[JHEP 04 \(2021\) 073](#)

$$\delta a_\tau = \frac{2m_\tau}{e} \frac{\sqrt{2}v}{\Lambda^2} \text{Re} [C_{\tau\gamma}]$$

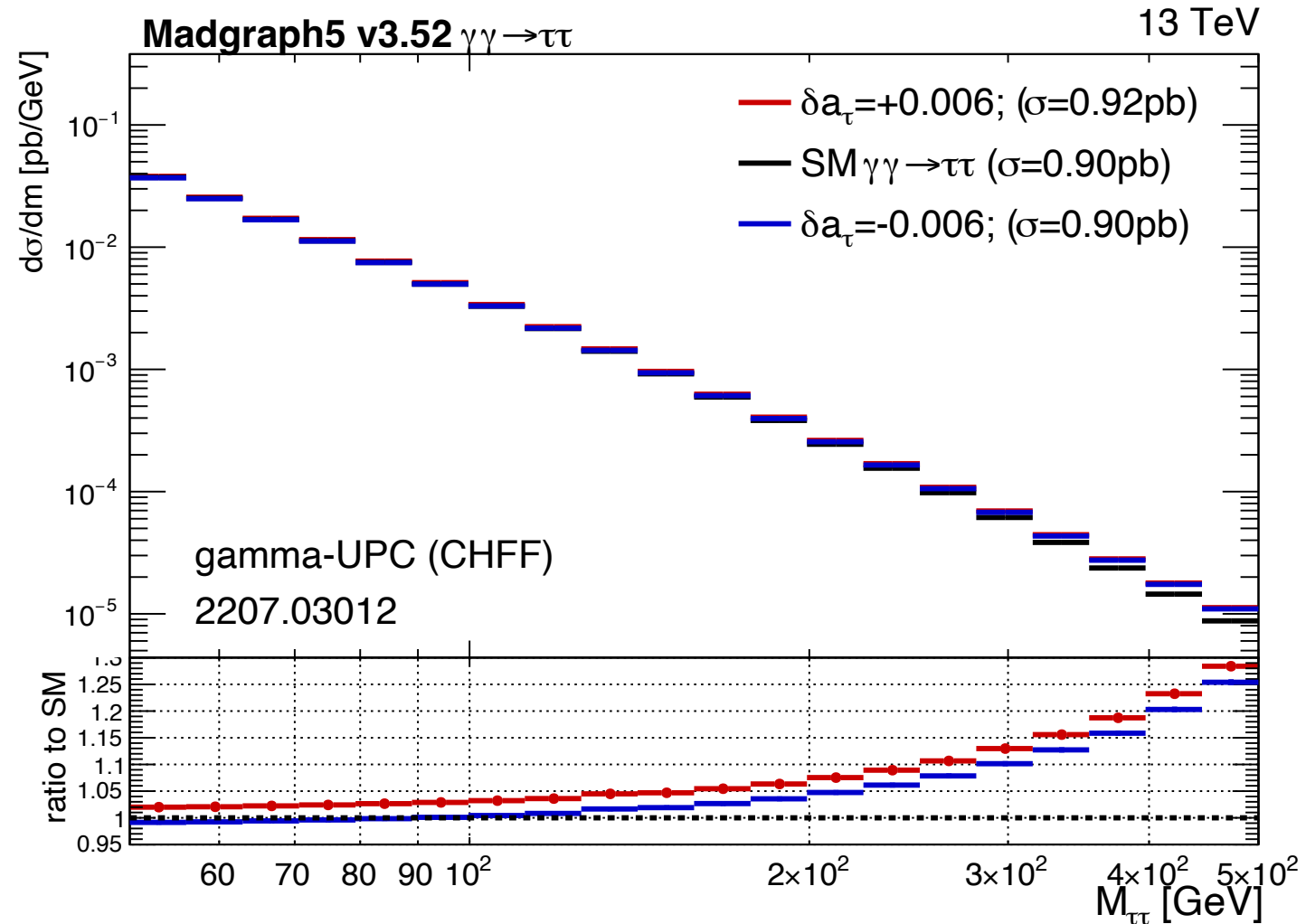
$$\delta d_\tau = \frac{\sqrt{2}v}{\Lambda^2} \text{Im} [C_{\tau\gamma}]$$

- where  $C_{\tau\gamma} = \left( \cos\theta_W C_{\tau B} - \sin\theta_W C_{\tau W} \right)$

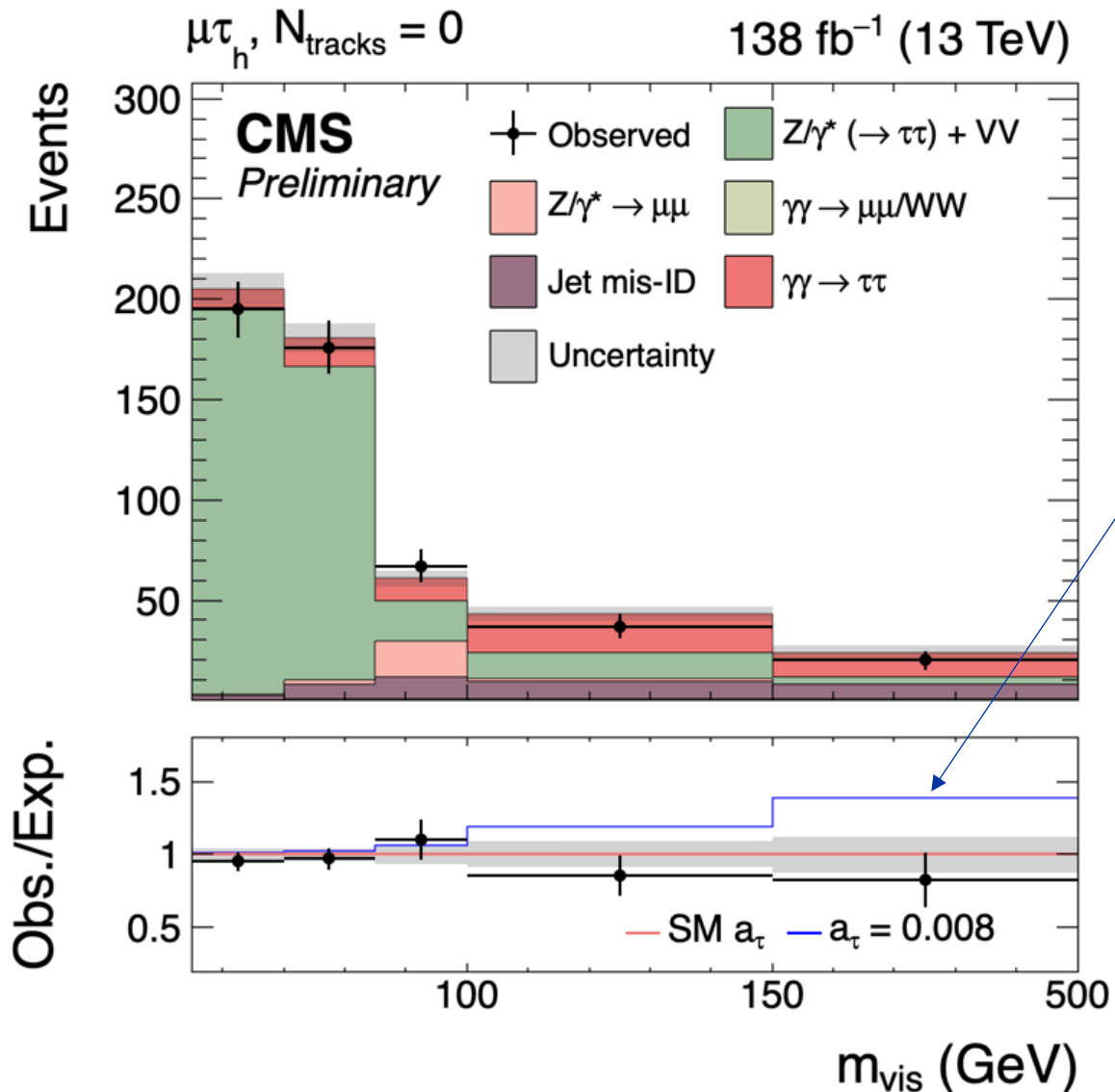
- Matrix element reweighting to model signal for BSM values of  $a_\tau$  and  $d_\tau$ , setting  $C_{\tau W}$  to 0 and scanning over  $C_{\tau B}$  without loss of generality

# How BSM physics in $a_\tau$ affects $\gamma\gamma \rightarrow \tau\tau$

- At large  $m_{\tau\tau}$ ,  $\gamma\gamma \rightarrow \tau\tau$  cross section increases with both positive and negative variations to  $a_\tau$
- The effect grows with  $m_{\tau\tau}$
- **We can constrain  $a_\tau$  by looking at the yield and  $m_{\tau\tau}$  distribution of the  $\gamma\gamma \rightarrow \tau\tau$  process**
- Expect better BSM sensitivity than with Pb-Pb runs because of higher  $m_{\tau\tau}$  range probed

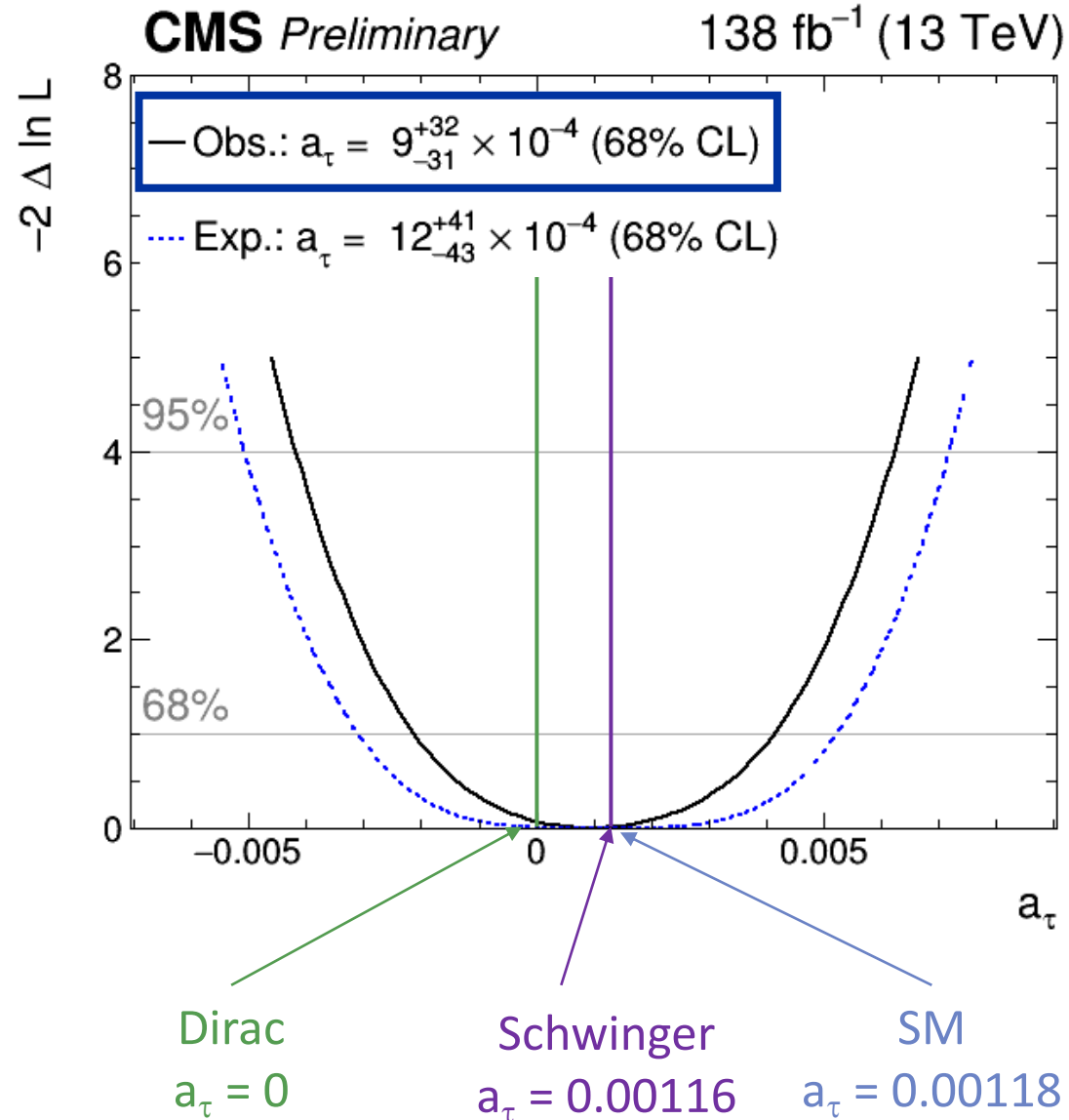


# How it translates in this analysis



- Changing  $a_\tau$  from its SM value modifies the  $\gamma\gamma \rightarrow \tau\tau$  prediction
- Differences between SM and BSM  $a_\tau$  scenarios increase with  $m_{\text{vis}}$
- $a_\tau$  can be constrained from the same  $m_{\text{vis}}$  distributions used to observe  $\gamma\gamma \rightarrow \tau\tau$
- $m_{\text{vis}} < 500$  GeV to remain far from new physics scale and preserve validity of EFT interpretation

# Extracting $a_\tau$

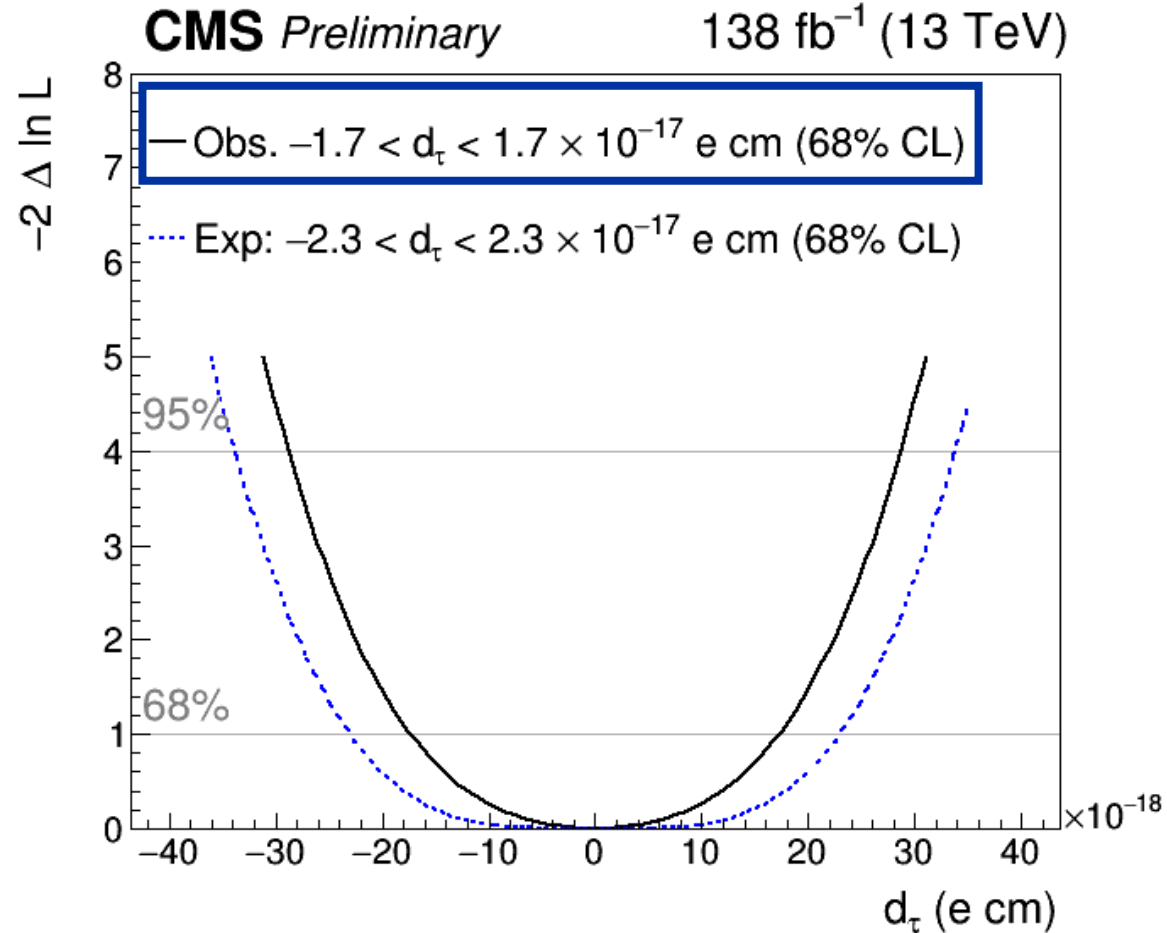


- Using  $m_{\text{vis}}$  distributions in the SR, perform negative log likelihood scan over  $\delta a_\tau$ , which modifies the signal shape and normalization
- In the  $m_{\tau\tau}$  range considered in this analysis, both  $\delta a_\tau > 0$  and  $< 0$  increase the signal prediction
- Observed  $\gamma\gamma \rightarrow \tau\tau$  deficit: tighter constraints than expected, **compatibility with SM**

**1 $\sigma$  uncertainty of 0.003**

**Only 3 times the Schwinger term!**

# Extracting $\tau$ EDM ( $d_\tau$ )

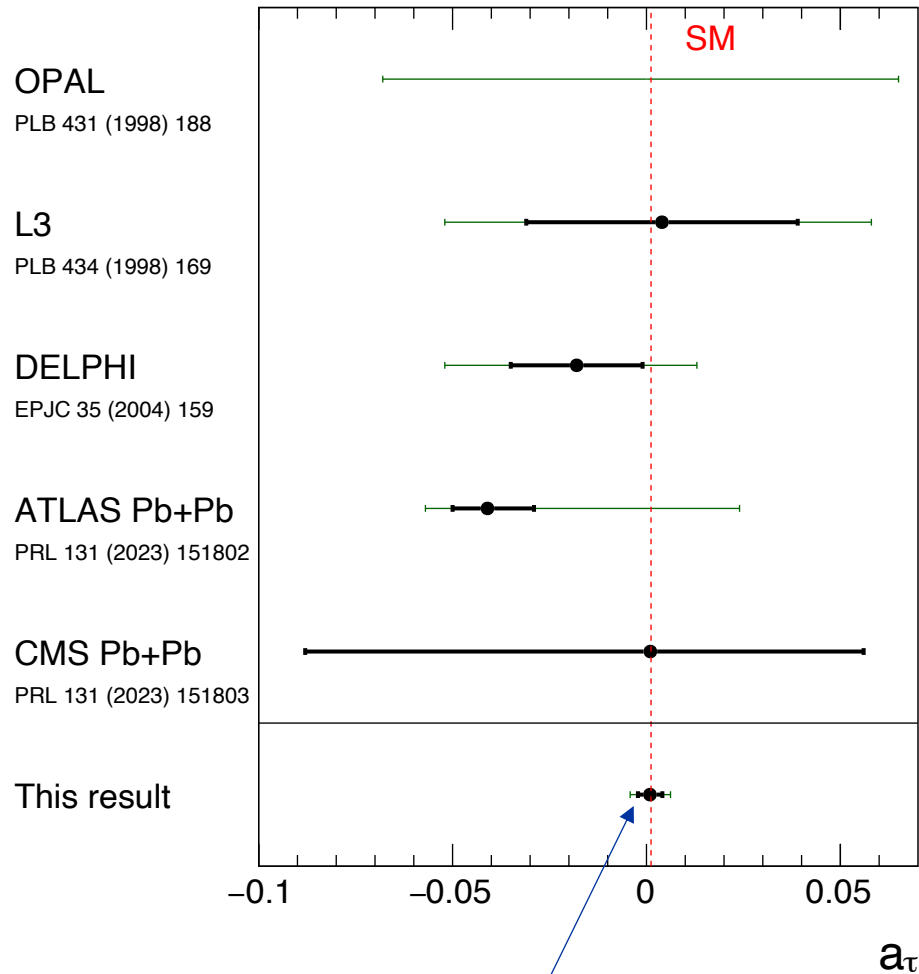


- BSM effects symmetric with sign of  $\delta d_\tau$
- In the  $m_{\tau\tau}$  range considered in this analysis, both  $\delta d_\tau > 0$  and  $< 0$  increase the signal prediction
- Observed  $\gamma\gamma \rightarrow \tau\tau$  deficit: tighter constraints than expected, **compatibility with SM**

# Comparing to previous results

**CMS Preliminary** 138 fb<sup>-1</sup> (13 TeV)

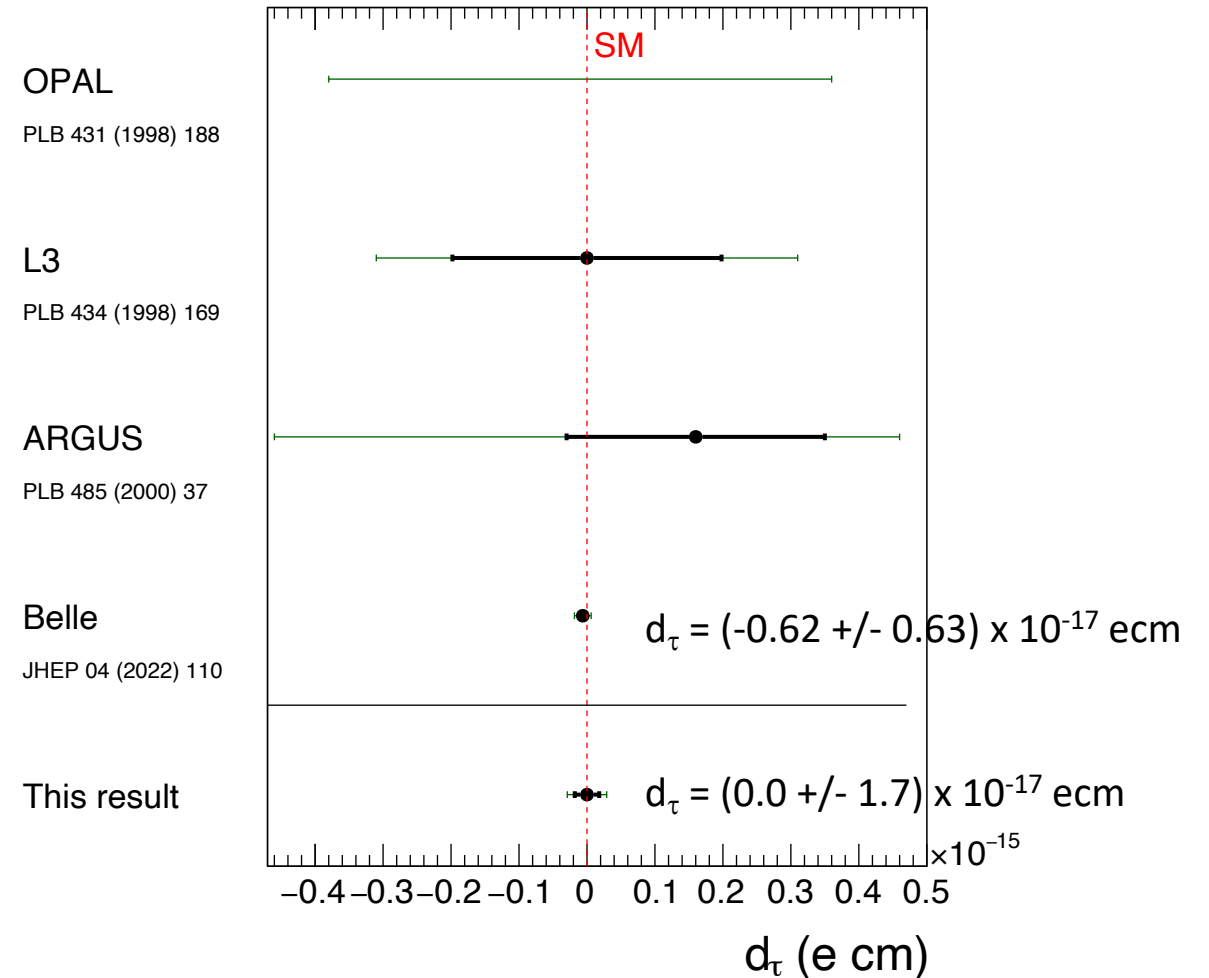
• Observed — 68% CL — 95% CL



Large improvement over LEP and LHC Pb-Pb

**CMS Preliminary** 138 fb<sup>-1</sup> (13 TeV)

• Observed — 68% CL — 95% CL



Approaching Belle precision



# The precision journey has just started...

DELPHI

**CMS pp**

OPAL

Approaching the

Pb-Pb LHC

Schwinger term!

More precision needed to  
probe BSM effects scaling  
with  $m_\ell^2$ ...

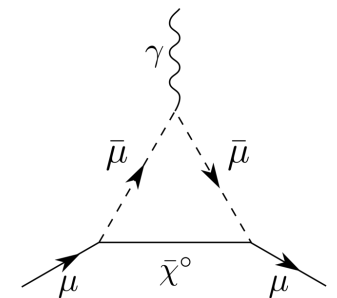
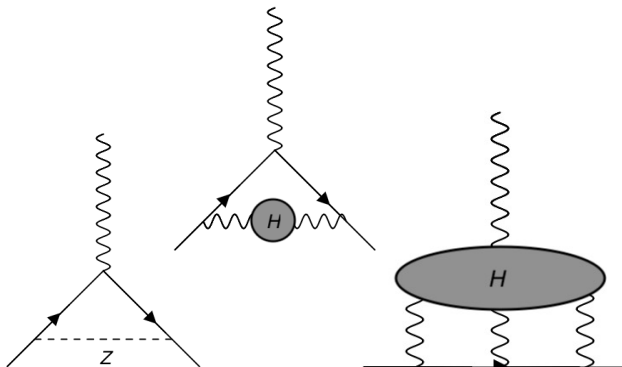
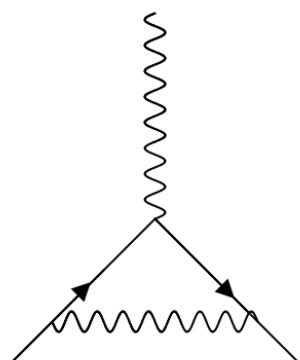
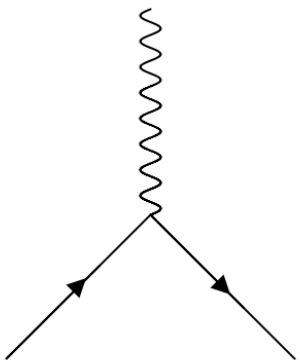
$a_\tau$  precision

*Dirac*

*Schwinger term*

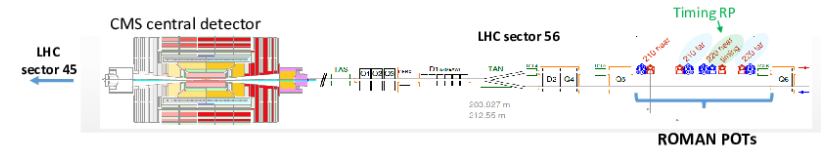
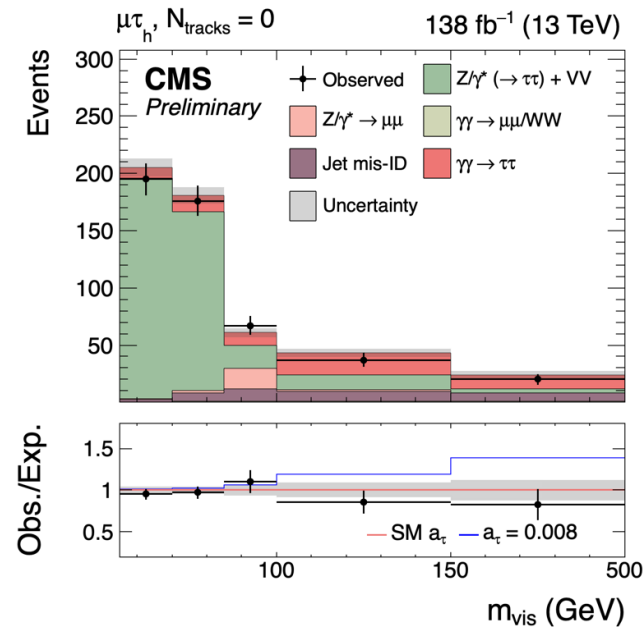
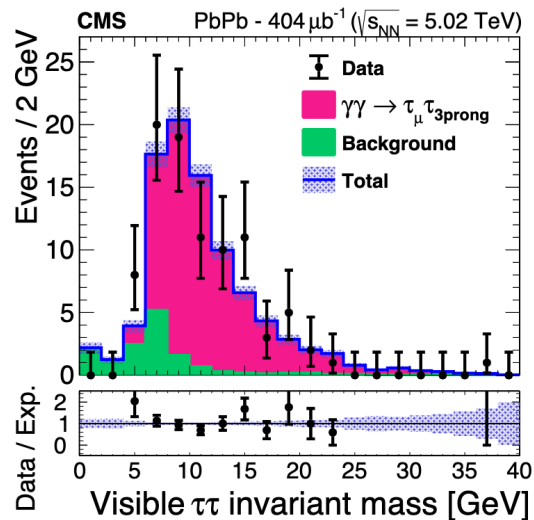
*Higher-order corrections*

*BSM effects?*



# ... and CMS will be a part of it

- Heavy ion runs
- pp runs with track counting
- pp runs with proton tagging



PPS approved for Run-4



The majority of CMS data has not been collected yet. Exciting complementary approaches for upcoming Runs!

# Conclusion

- Thanks to the excellent tracking performance of the CMS detector, we can isolate photon-induced events in ultraperipheral proton-proton collisions without tagging protons
- **The CMS Collaboration has observed, for the first time,  $\gamma\gamma \rightarrow \tau\tau$  events in pp runs**
- These events were used to constrain the tau electromagnetic moments with an EFT approach

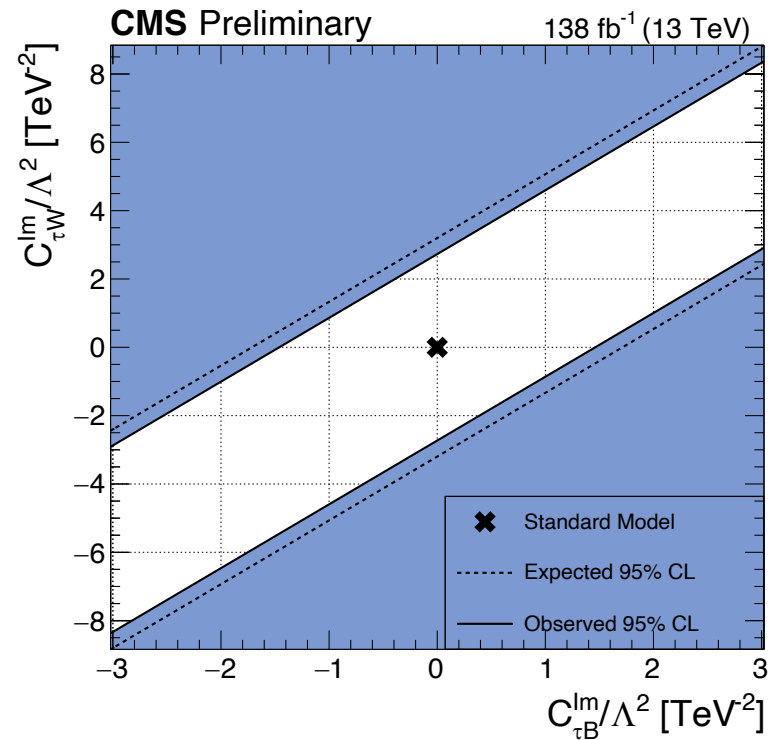
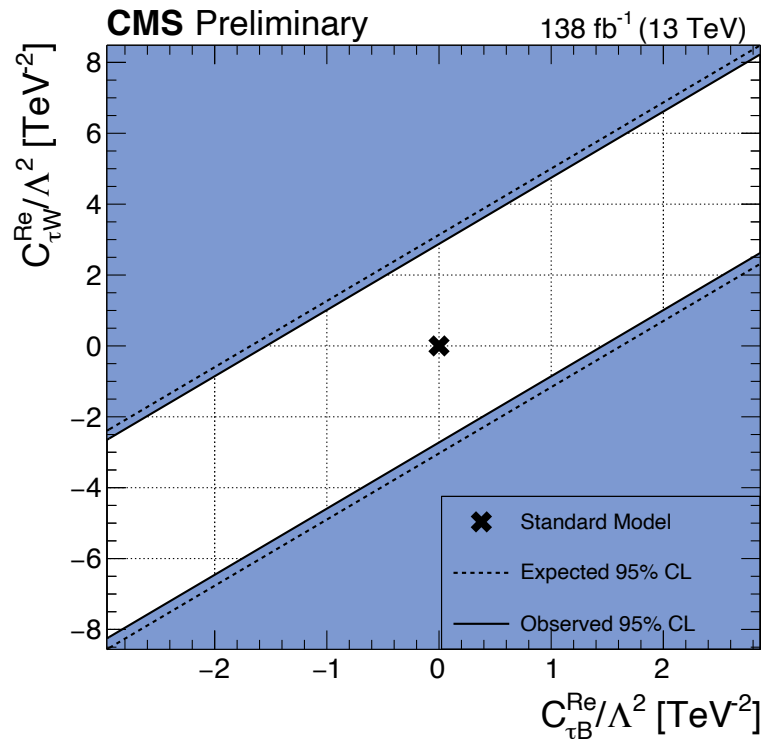
$$a_\tau = 0.0009 +0.0032/-0.0031 \text{ at 68\% CL}$$

$$-0.0042 < a_\tau < 0.0062 \text{ at 95\% CL}$$

- **Improving previous constraints on tau g-2 by a factor of ~5** (PDG:  $-0.052 < a_\tau < 0.013$  at 95% CL) and approaching the precision of the Schwinger term (0.00116)

# Backup

# Constraints on Wilson coefficients



- $-1.68 < \text{Re}(C_{\tau B})/\Lambda^2 < 1.62 \text{ TeV}^{-2}$
- $-3.03 < \text{Re}(C_{\tau W})/\Lambda^2 < 3.13 \text{ TeV}^{-2}$
- $-1.71 < \text{Im}(C_{\tau B})/\Lambda^2 < 1.71 \text{ TeV}^{-2}$
- $-3.20 < \text{Im}(C_{\tau W})/\Lambda^2 < 3.20 \text{ TeV}^{-2}$